Region 2
UNIVERSITY TRANSPORTATION RESEARCH CENTER

Final Report

Development of a Portable Petroleum By-Products Chemical Sensor: Phase III and IV

NYS-DOT Project C-02-08

Prepared by

Professor Michael A. Carpenter
College of NanoScale Science and Engineering
University at Albany, SUNY
Albany, NY 12203

&

Professor Marina A. Petrukhina
Department of Chemistry
University at Albany, SUNY
Albany, NY 12203

August 21, 2009

Disclaimer

The contents of this report reflect the views of the author who is responsible for the facts and accuracy of the data presented herein. The contents do not necessarily reflect the official views or policies of the New York State Department of Transportation, the United States Department of Transportation, or the Federal Highway Administration. This report does not constitute a standard, specification, regulation, product endorsement, or an endorsement of manufacturers.

TECHNICAL REPORT STANDARD TITLE PAGE

1. Report No.	2. Government Accession No.	3. Recipient's Catalog No.

4. Title and Subtitle
Development of a Portable Petroleum By-Products Chemical Sensor: Phase III and IV

5. Report Date
August 21, 2009

6. Performing Organization Code

7. Author(s)
Dr. Michael Carpenter & Dr. Marina A. Petrukhina, University at Albany, SUNY

8. Performing Organization Report No.

9. Performing Organization Name and Address
College of NanoScale Science and Engineering
University at Albany, SUNY
Albany, NY 12203

10. Work Unit No.

11. Contract or Grant No.
55657-02-20 & 55657-05-19

12. Sponsoring Agency Name and Address
NYS Department of Transportation
50 Wolf Road
Albany, NY 12232

University Transportation
Research Center-Region 2
138th Street & Convent Ave
New York City, NY 10031

13. Type of Report and Period Covered
Final Report
May 1st, 2007 - March 31st, 2009

14. Sponsoring Agency Code

15. Supplementary Notes

16. Abstract

Semiconductor quantum dots (QDs) are considered to have potential for chemical sensing application because of their high surface to volume ratio and unique size tunable properties like photoluminescence (PL). However, our study revealed for the first time that optical sensing process of nanoparticle based material is complicated, involving a lot of issues like how to assemble QDs without losing their original properties, nanoparticle associated light/matter interaction change and interference of analyte absorption in the film, how to achieve desired sensitivity, selectivity and stability for sensors, and etc. We carried out systematic researches on these from CdSe synthesis, surface functionalization, construction of QDs into sensible host media, sensing studies. Many improvements have been made which required overcoming various obstacles and the development of novel approaches and methods. As a result, we have achieved the lowest detection limit for hydrocarbons, ~10 ppm xylenes, within QD based sensing technologies, a monotonic detection range which spans over three orders of magnitude in analyte concentrations, which is a prerequisite for any sensor in real world applications. We also achieved selectivity for BTX that differs by only one methyl group, which can be combined into QDs sensor array with different QD sizes and temperature gradient for realization of complete selectivity.

17. Key Words	18. Distribution Statement
Semiconductor, Nanoparticle, Quantum Dots, Chemical, Optical, Spectroscopy, Hydrocarbon	

19. Security Classif (of this report)	20. Security Classif. (of this page)	21. No of Pages	22. Price
Unclassified	Unclassified	36	

Form DOT F 1700.7 (8-69)

Development of chemical sensors with semiconductor CdSe quantum dots

Abstract

Semiconductor quantum dots (QDs) are considered to have potential for chemical sensing application because of their high surface to volume ratio and unique size tunable properties like photoluminescence (PL). However, our study revealed for the first time that optical sensing process of nanoparticle based material is complicated, involving a lot of issues like how to assemble QDs without losing their original properties, nanoparticle associated light/matter interaction change and interference of analyte absorption in the film, how to achieve desired sensitivity, selectivity and stability for sensors, and etc. We carried out systematic researches on these from CdSe synthesis, surface functionalization, construction of QDs into sensible host media, sensing studies. Many improvements have been made which required overcoming various obstacles and the development of novel approaches and methods. As a result, we have achieved the lowest detection limit for hydrocarbons, ~10 ppm xylenes, within QD based sensing technologies, a monotonic detection range which spans over three orders of magnitude in analyte concentrations, which is a prerequisite for any sensor in real world applications. We also achieved selectivity for BTX that differs by only one methyl group, which can be combined into QDs sensor array with different QD sizes and temperature gradient for realization of complete selectivity.

1. Introduction

The testing of soil samples is performed during all phases of construction (planning, building, and post construction). This is done to ensure that the soil removed is not contaminated and when construction is complete, ensure that the environmental impact of the structure is minimal. Commonly soil samples are extracted and sent to an analytical lab for testing of pollutants (hydrocarbons and metals). The direct impacts of this process are time consuming and expensive, however the expense will also include construction delays which may eventually lead a construction project out of budget and miss its deadlines. A portable soil sensor for the detection of known tracer organics for gasoline, diesel fuel, and PCB's (polychlorobiphenyls) will reduce the number of samples sent to an outside lab, thus reducing the overall cost of construction projects. We propose to tailor design nanoparticle based chemical sensors for the sensitive, selective and field portable analyses of soil samples for petroleum spill indicating hydrocarbons (such as benzene, toluene, ethyl-benzenes, xylenes, PCBs, trichloroethylene). An optical and an electrical based transduction mechanism will utilize nanoparticles as the sensing layer, and to achieve ppb sensitivity we will integrate a preconcentrating device coupled to the sample degassing chamber.

The high pay off of the proposed research lies in the future target applications of nanoparticle based chemical sensors. One example is for monitoring benzene, toluene, ethyl benzene, and xylenes (BTEX) for applications in groundwater well networks or soil sample analysis. BTEX compounds are indicative of petroleum by-product contamination and currently the US-EPA has regulations for performing a standardized test of groundwater and soil samples using modern analytical laboratory equipment. Off-site analytical lab testing of both groundwater and soil samples are a significant expense of environmental monitoring and cleanup operations throughout the federal and state level

Superfund program. Since its inception in 1986, the New York State Superfund program alone has identified, characterized and placed a total of 1,714 sites on the Registry of inactive hazardous waste disposal sites. Details of these sites are as follows:[1]

- A total of 934 sites have been identified that require remediation; growth is approximately 30 sites/yr
- 215 of these sites require long-term operation, maintenance, and monitoring (OMM) to ensure that remediated sites continue to protect the public health (growth of OMM sites is approximately 30/yr)
- In the 1999/2000 fiscal year approximately $9 million were spent on site investigation, remediation investigation and OMM, all of which required extensive sampling, monitoring and analysis of soil and groundwater samples
- To date funds spent or obligated to be spent total approximately $4.61 billion: $3.01 billion by responsible parties, $1.05 billion by New York State and $554 million by the federal government

It is clear that significant cost savings at both the state and federal levels would occur if chemical sensors integrated with pattern recognition techniques were developed for continuous on-site environmental monitoring, specifically for analyzing groundwater well and soil samples. Future advances and phases of the proposed research program would likewise integrate in-situ remediation processes in the event of a detected pollution plume and lead to far less expensive cleanup procedures.

NYS-DOT spends approximately $10-12 million on the testing of soil and groundwater samples, which does not include the NYC-DOT which must have a comparable if not larger budget for such testing.[2] By moving the majority of these tests from an off-site analytical lab, to a field portable device the overall cost of construction budgets will be significantly lower and construction projects will have less delays due to untimely analytical lab reports.

Semiconductor nanoparticles attract great interest for applications in materials science and nanotechnology[3,4,5,6,7] due to the quantum confinement effect. These nanoparticles show special physical and chemical properties when their core size is close to or smaller than the dimensions of the exciton Bohr radius of the material. Such unique properties of semiconductor nanoparticles, also known as quantum dots (QDs), have made them very promising for various practical applications including electronics, [8,9,10] optics, [11] chemical [12, 13] and biological sensors. [, 14] A distinctive characteristic of these nanoparticles is that their photoluminescence (PL) properties have been shown to strongly depend on their surface environment. [15, 16] Our interests are focused on developing QD-based sensing materials, which have the ability to provide multiple levels of selectivity through the tailored design of both the host matrix and the QD itself for a specified sensing application. Therefore, we have initiated a series of studies on the use of surface modified CdSe quantum dots for the selective and sensitive detection of aromatic hydrocarbons (HCs).

We proposed to produce surface modified QDs, which utilize both stabilizing (trioctylphosphine oxide, TOPO and stearic acid, SA) and surface modifying (benzoic acid (BA), pentafluorobenzoic acid (FBA) or naphthylamine (NA)) reagents [12]. Traditionally, monodispersed and highly luminescent QDs are synthesized at elevated

temperatures using coordinating organic capping agents such as trioctylphosphine and trioctylphosphine oxide (TOP/TOPO). [17] The latter prevent aggregation and preserve optical properties of QDs and therefore are referred to as surface protecting or "stabilizing" groups. Additional surface-bound functional groups may allow integration of QDs into matrices or materials or provide special characteristics, like enhanced sensing properties. [10,11] Typically, these surface groups are introduced by post-synthesis ligand exchange, [] as the high-temperature QD growth methods are not compatible with most organic functional groups. However, generally this process suffers from incomplete surface exchange and ligand coverage. More often, the photoluminescence is quenched due to aggregations of QDs [18] or generation of surface defects [19] occurring during ligand exchange procedures. Photoluminescence may also oscillate due to adsorption and desorption of the newly grafted surface groups. To overcome these problems, we attempted to do in-situ surface functionalization for the QDs with surface modifying groups, BA, FBA, or NA not via ligand exchange, but during the synthesis of the QDs. The presence of the above surface bound agents was confirmed by NMR spectroscopy [12].

Before many applications can be realized, QDs must be functionally integrated into devices, and controlled integrations of them into preferred structures appears to be an essential prerequisite for the realization of high-performance optical and opto electronic devices. For the preparation of QD-based polymer composites two methods are generally used: a) in situ synthesis of QDs in either a polymer solution [20] or within a film [21] and b) ex situ synthesis of QDs followed by their subsequent incorporation into either monomer or polymer solution or a film. [22] Usually the PL quantum yield of in situ synthesized QDs does not exceed 16 % [23] due to the low temperature synthesis required by the polymers, which results in low optical quality QDs. Numerous attempts have been made to fabricate uniform 2D and 3D nanoparticle-based multilayers by using such diverse approaches as self-assembly,[24] colloid crystallization, Langmuir-Blodgett technique, electrostatic interactions. [25] We have adopted and developed different techniques to create desired QD based material systems, including controlled drop casting, [12,13] in-situ polymerization of CdSe core dots with monomers, [26] in-situ surface functionalization to afford highly luminescent QD solutions followed by layer-by-layer building up of QD multilayered thin films,[27] and integration of QDs directly onto nanotube array, like anodic aluminum oxide (AAO). [28] For the layered approach, we used 11-hydroxyundecanoic acid (11-HUDA) to perform functionalization of CdSe quantum dots in situ during QD synthesis. Thus prepared stable and highly luminescent CdSe QDs are then utilized in fabrication of layered thin films on glass or silicon substrates through a covalently bonded layer-by-layer formation. In this case, the ligand exchange is avoided and the high quantum yield and stability of the CdSe QDs is preserved due to the absence of thiols on the particle surface. [27]

Controlled drop-casting method enables us to fabricate surface modified and unmodified QD/PMMA films that are sensing workable. We achieved a detection limit of 15 ppm for xylenes, which is the lowest within the results reported in the literature [12,29,30]. We also observed 2-3 times grater selectivity for xylenes than that of toluene. Xylenes detection limit is found to improve with variation of the surface group in an order of bare (unmodified), BA, NA, and FBA. The introduction of F-substituents to the π-system of benzoic acid proffers its electron-deficient properties, which should

influence the surface interaction of QDs with the targeted HC molecules, while NA has an amino surface bound group which differs from the carboxyl surface bound group of BA and FBA. Furthermore, NA has two aromatic rings which potentially provides an extra site for interaction with the HC target species. [12,13]

However, both PL enhancement and quenching take place for the QD films with exposure from low to high levels of HCs, in agreement with the inconsistent PL response reported in the literature [29,30]. We performed a detailed study on these effects and determined that PL enhancement results from QD and analyte interaction, while PL quenching is from physical wetting effect due to absorption of high amount HC in the film. This study revealed for the first time that optical sensing process of nanoparticle based material is complicated, involving a lot of issues like how to assemble QDs without losing their original properties, nanoparticle associated light/matter interaction change and interference of analyte absorption, how to achieve desired sensitivity, selectivity and stability for QD sensors, and etc. [31]

Our finding that porous and rough film structures is a desired structural property for optical sensors inspired our introduction of AAO as a quasi photonic crystal (PC) platform for QDs dispersion, which offers two advantages for QD based sensing. First, AAO intensifies QD photoluminescence (PL) thus increasing the sensing response toward analyte exposures owing to both the redistribution of high intensity near-fields for more efficient excitation of QDs and strong scattering effects for enhanced extraction of the resulting QD emission. Rough surfaces are widely used in solar cells to enhance light capture. Second, the nanotubes of AAO retards the limiting effect of film wetting and resultant PL inversion and desensitization suffered from QDs or QDs/polymer cast on non-porous substrates under exposures to increased levels of analytes and as a result PL enhancement prevails. [28] The combination of QDs and nanotube arrays has enabled the development of QDs based materials for sensing applications across large dynamic ranges, for example, 10 to 9400 ppm for xylenes. Moreover, placing the AAO/Au sample on a Si support with different surface coatings, like Au, can further improve PL and the corresponding sensing responses. We have also performed a series of studies based on this new sample structure, specifically we have determined the sensing dependence on the separation distance of the phenol group(within the enhancing ligand) to the QD surface is studied with the result showing that the longer PHA yields the highest PL and sensitivity to xylenes. [32]

Of specific concern through our studies is the PL stability of the QD based hydrocarbon sensing films. While the core (CdSe) based QDs have been shown to be rather sensitive and selective, they also suffer from PL instabilities caused by oxidation of the surface layers, leading to nearly complete PL quenching within 3 weeks time. In order to pursue QD based hydrocarbon sensing films with much longer PL stability we have investigated CdSe/ZnS core/shell QDs based films in order to demonstrate improved sensitivity and stability compared to core dots. **These studies have shown the sensitive and selective detection of hydrocarbons over nearly 9 months time and are very promising for future studies.** In the future, combination of surface modified core/shell QDs and nanotube array along with surface coating manipulation on Si support is expected to further improve the sensor performances for real word applications.

The remaining body of this report details the experimental procedures/protocols for the work performed in this program and details results pertaining to the development of

new chemistries to functionalize the QD surface, new film deposition procedures including a novel layer by layer synthesis method, detailed studies on how the QD host material(including polymer hosts, and inorganic hosts) affects the detection limits and the detection range of the sensing material, fundamental studies on the surface ligand length and the corresponding sensing methods, and lastly the characterization and use of core shell QDs deposited on inorganic host materials for **large dynamic detection range** and **9 month long** stability tests. The report finishes with a conclusion section which briefly summarizes the results.

2. Experimental

Chemicals

Technical grade (90%) trioctylphosphine oxide (TOPO), technical grade (90%) trioctylphosphine (TOP), cadmium oxide (99.99+%), anhydrous methanol (99.8%), anhydrous chloroform (99%), deuterated chloroform (99.8% atom D) were purchased from Aldrich. Selenium powder (99.9%) was purchased from Ventron. 1-hexadecylamine (HDA), benzoic acid (BA), stearic acid (SA), chloroform, methanol were purchased from Acros. Pentafluorobenzoic acid (FBA) was purchased from SynQuest Laboratories. Poly(methyl methacrylate) (PMMA) was purchased from Scientific Polymer Products, Inc. ethylene glycol dimethacrylate (98%), AIBN (2,2'-azo-bis(isobutyronitrile)), 2-naphthylamine (NA) were purchased from Aldrich. Selenium powder (99.9%) was purchased from Ventron. 1-hexadecylamine, benzoic acid (BA), stearic acid (SA), lauryl methacrylate (96%), chloroform, methanol were purchased from Acros. n-hexyl methacrylate was purchased from Scientific Polymer Products, Inc. Stearyl methacrylate was purchased from TCI America. Behenyl methacrylate was purchased from Monomer-Polymer & Dajac Labs, Inc. 1,6-hexamethylene diisocyanate (HMDIC) (99%), 3-aminopropyltriethoxysilane (APTES) (99%), methanol were purchased from Acros Organics. 11-Hydroxyundecanoic add (11-HUDA) and 16-hydroxyhexadecanoic (16-HHDA) acids were purchased from Oakwood Products.

Synthesis and surface-functionalization of CdSe Quantum Dots

The CdSe quantum dots with stabilizing (TOPO and stearic acid, SA) and surface enhancing groups (choice of benzoic acid (BA), pentafluorobenzoic acid (FBA), 4-phenylbutanoic acid (PBA), 6-phenylhexanoic acid (PHA)) have been synthesized according to procedures modified from those previously published. In a typical reaction procedure CdO (0.103 g, 0.8 mmol) and stearic acid (0.911 g, 3 mmol) were placed into a three-neck flask and heated to 150˚C under a dinitrogen flow for the synthesis of unmodified QDs, while the respective addition of benzoic acid (0.048 g, 0.4 mmol) or pentafluorobenzoic acid (0.085 g, 0.4 mmol) to this mixture was utilized for the synthesis of the surface modified QDs. After CdO was completely dissolved, the mixture was allowed to cool to room temperature and 6 g of TOPO and 3 g of HDA were added to the flask. The mixture was then heated to *ca.* 300˚C under a dinitrogen flow. At this temperature a Se solution containing 0.632 g of Se powder in 4.2 mL of TOP was swiftly injected. After the injection, the temperature was reduced to 250˚C. At the desired QD size, the reaction was stopped by removal of the heating bath. Aliquots were mixed with methanol and the precipitated QDs were separated by centrifugation. In order to remove

unbound reagents, the process of dispersion in methanol and centrifugation was repeated several times.

Substrate preparation

The glass substrates (VWR scientific International) were initially washed with dilute HCl and soap solutions to remove the surface adhered contaminants. The substrates were then immersed in a 5N NaOH aqueous solution overnight for making the surface hydrophilic. Finally, they were washed with distilled water and ethanol and dried under a N_2 stream. Commercially purchased single-crystal (111) Si wafers were diced into 15 mm×25 mm chips. Prior to use, they were cleaned by immersion in a series of ultrasonically agitated solvents (acetone, toluene, acetone, ethanol, H_2O) for 15 s each followed by 60 s immersion in ultrasonically agitated 2 % Alkonox solution, then rinsed with H_2O and ethanol. The wafers were kept for 15 min in dichloromethane and then immersed in a mixture of NH_3 (25 vol. %), H_2O_2 (30 vol. %), and distilled water in the volume ratio of 1:1:5 at 70 °C for 20 min. Afterwards, the wafers were washed with distilled water and dried in a stream of N_2. The amino-terminated monolayers were obtained by dipping the freshly cleaned silicon wafers into a 2 wt % solution of (3-aminopropyl)triethoxysilane (APTES) in toluene for 5 min at 70 °C. After that the wafers were washed five times with toluene, dried in a stream of N_2, and used immediately.

Sensing film development

The QDs, prepared as described above, have been encapsulated into PMMA matrices. Films of a micron-range thickness were prepared by drop coating a QD/PMMA solution onto Si-substrates, with the resulting droplet left to slowly evaporate in a covered dish overnight. The QD loadings for each of the QD-PMMA films used in this study are listed in Table 1. The drop-coated films were observed to undergo a QD phase separation from the polymer matrix with an increase in QD loading of the polymer host. This is due to the limited miscibility of TOPO covered QDs within the PMMA matrix [33, 34, 35, 36, 37, 38, 39]. However, the non-uniformity did not significantly affect the hydrocarbon (HC) sensing characterization, as the optical properties of the QD films were collected and averaged over a 5 mm-diameter spot size. The reproducibility of producing QD-polymer films via the drop coating technique was addressed by depositing 15 individual QD-FBA/PMMA films from the solution, and comparing the PL for all 15 films. Furthermore, the xylenes sensing properties were measured for 5 of these films to examine the consistency of their detection characteristics.

Polymerization

We adapted the procedure described by Lee at al. 0.076 g of unpurified CdSe QDs were mixed with 0.7 g of each monomer and TOP (42 µl), and the mixture was stirred for 15-30 minutes at room temperature. Then, 1.25 mL ethyleneglycol dimethacrylate crosslinker was added to the QD-monomer solution. This was followed by stirring for an additional 10-30 minutes. The higher concentrations of QDs required more time to mix. Then, azobisisobutyronitrile (AIBN) radical initiator (<1% (w/w)) was added, and the mixture was stirred for another 5-15 minutes. The final solution was then transferred either to a 30 mm x 5 mm (length x diameter) glass tube or between two optical flats and polymerized in an oven at 75º C for 2 h in air. A high-clarity QD-polymer composite rod

and films of 1 mm thickness were then removed from the glass mold or from the optical flats. The thickness was controlled by insertion of an optical flat (1mm thickness) between two other optical flats.

Fabrication of multilayered films

The film fabrication process was carried out inside a purge box under a N_2 atmosphere. The pre-treated glass and silicon substrates were immersed in 5 wt % solution of hexamethylene diisocyanate (HMDIC) in toluene at room temperature for 6 h followed by rinsing with toluene under ultrasonication. The isocyanate-bearing substrates were then immersed in the THF solutions containing CdSe QDs (10 mg, 10 mL) for 4 h followed by rinsing with THF under ultrasonication. Thus a monolayer of CdSe QDs on the substrate was formed. This process was repeated in order to form three-dimensional multilayers on different substrates.

Integration of QDs onto AAO

In order to realize self-assembly like dispersion of QDs on AAO with controlled spot size of ~ 6 mm, several measures are required to be taken. First, AAO of ~200nm pore size in this work is selected to ensure less hydrophobic AAO surface than toluene dissolved QD solution to control drop coating without lateral spreading and some longitudinal leaking into the nanotubes (constrained by surface tension) since hydrophobic property of AAO surface is dependent on the size of pores filled with hydrophobic air. Second, AAO is suspended on two glass or silicon pieces placed within a glass Petri dish to avoid other sources induced droplet spreading like electrostatic force seen with the droplet, if AAO is otherwise directly placed on the dish. Here, it is considered that the weight of droplet on the suspended AAO of ~60 μm thickness induces some deformation of AAO and helps constrain the droplet from spreading. Third, after slowly delivery of QD solution volume (~ 5μl) with a syringe to form a non-spreading droplet, the dish was loaded with a couple of toluene droplets on its bottom surface and sealed with a parafilm and then with cover for QD slowly self-assembling in toluene environment overnight or longer. The utilized CdSe/ZnS in toluene is from Evident technology, and AAO template is ordered from Whatman.

Characterization

Uv-vis absorption spectra were recorded on a Varian Cary Uv-vis spectrophotometer. The band gap energy was determined by analyzing the absorption data using the method outlined by Yu et al.. These values were then used to estimate the diameter of the QDs. Photoluminescence (PL) spectra of the QD solutions were acquired using a Varian Eclipse spectrofluorometer. High-resolution transmission electron micrographs were obtained on a JEOL 2010F transmission electron microscope (TEM) operating at 200 keV. The TEM samples were prepared by placing a dilute solution of QDs in chloroform onto carbon-coated copper grids and allowing them to dry in a vacuum desiccator overnight. High resolution TEM and X-ray diffraction data confirmed a high degree of crystallinity of the QDs. The QD diameters and size distributions determined through TEM particulate analysis were consistent with those obtained from the absorption spectra analysis and are listed in Table 1.

^{1}H and ^{19}F NMR spectroscopy data were used to analyze the degree of attachment of the surface groups to the QDs. The purified QDs were dried in the dark for 2 hours under vacuum at 50ºC to remove any remaining volatile organics. The QDs (0.020 g) with BA or FBA groups on the surface were then dissolved in 1 mL of $CDCl_3$. ^{19}F NMR spectra were obtained using a Varian Gemini 300 MHz spectrometer. ^{1}H NMR spectra were obtained using a Bruker Avance 400 MHz spectrometer. Chemical shifts for ^{1}H NMR spectra are reported as parts per million relative to tetramethylsilane, while the ^{19}F NMR spectra are reported relative to $CFCl_3$.

The AFM images of the monolayer of QDs on glass were obtained using a Veeco Explorer AFM in a tapping mode. Photoluminescence (PL) spectra were acquired using a Fluorolog-3 with FluorEssence (Jobin Yvon Horiba) spectrofluorometer. FTIR spectra (16 scans with 4 cm^{-1} resolution) were recorded using a Spectrum 100 FTIR spectrometer (Perkin-Elmer) in an attenuated total reflectance mode for QDs powders.

Photoluminescence (PL) spectra were acquired using a Fluorolog-3 with FluorEssence (Jobin Yvon Horiba) spectrofluorometer. FTIR spectra (16 scans with 4 cm^{-1} resolution) were recorded using a Spectrum 100 FTIR spectrometer (Perkin-Elmer) in an attenuated total reflectance mode for QDs powders.

Hydrocarbon exposure testing

The sensing films were rigidly mounted in a stainless steel testing chamber with an internal volume of 20 cc. A Varian Eclipse spectrofluorometer was employed to characterize the PL properties of the sensing films. The spectrometer utilized a bifurcated fiber optic accessory for both delivery of the 350 nm excitation light to the film surface, via a vacuum compatible fitting, and collection of the resulting emission for detection. A HC vapor producing system using a glass bubbler and an Environics gas mixing system generated HC vapor concentrations adjustable from several ppm to several percent by changing the gas flow through the bubbler. The total pressure of the bubbler was monitored and maintained at 850 torr, while the bubbler was under ambient room temperature conditions. Thermal measurements of the bubbler during the experiments indicated that the temperature fluctuated by ~1°C, and thus the toluene and xylenes concentrations delivered to the testing station only varied by ~3-5% throughout the testing period. The HC sensing capabilities of the films were characterized by monitoring the peak PL intensity change of the QDs while the gas environment of the test chamber was varied from pure N_2 to a HC/N_2 mixture through the computer controlled vapor-producing system, with 5 minute half cycles used for each exposure test. The total test gas flow, pressure and temperature within the testing chamber were maintained at 1200 sccm, 760 Torr and ~25 ˚C, respectively.

3. Results and discussions

A. Tailor Designed CdSe Quantum Dots for the Selective Detection of Hydrocarbons

In order to achieve selective and sensitive sensing of hydrocarbon (HC) species, we proposed to tailor CdSe QDs surface with aromatic ligands to introduce additional pi-pi staking interaction with HCs. However, ligand exchange for the QD surface functionalization from conventionally synthesized QDs is impossible, so we performed a simultaneous QD synthesis along with surface engineering, where a combination of stabilizing ligands (TOPO, TOP, HAD, SA) and a choice of "surface enhancing" groups (e.g. FBA) was attached to the surface of CdSe QDs. The attachment of BA to QD surface is confirmed by the chemical shift of BA ^{1}H NMR peaks from solution of QD-BA in $CDCl_3$ relative to that of BA in $CDCl_3$ (Fig. 1). The surface coverage is estimated to be 1 molecule of BA per 12 molecules of TOPO for each quantum dot. Attachment of FBA molecules to the QD surface is also confirmed when the ^{19}F-NMR spectrum of QDs with FBA on the QD surface is compared with that of protonated FBA [40].

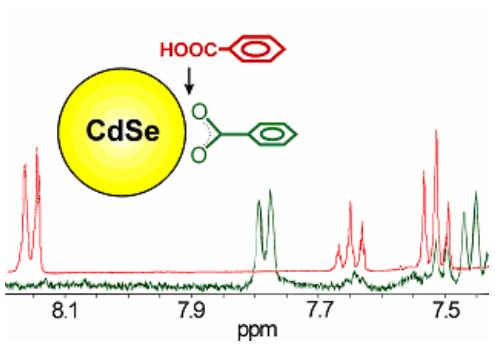

Fig. 1 ^{1}H NMR spectra of BA (red) and CdSe-BA (green) in $CDCl_3$.

Next, we established a method to mix and cast QD/PMMA solution onto a silicon substrate with a careful control of liquid volume delivery by micro syringe and leave the droplet drying in solvent environment overnight. By this way, the QDs were encapsulated into PMMA matrices to form porous nanocomposite films (see Table 1 for the loadings), followed by photo-treatment under irradiation of 350 nm light and a 1200 sccm flow of N_2 for subsequent HC exposures. Figure 2 shows that the peak PL intensities of the three QD/polymer films became stable in less than 1 to 2 hrs of photo-curing with intensity increase or decrease by extent of 3-34 %, which are comparable to those

Table 1. QD sizes and concentrations utilized in the PMMA films

	CdSe-SA	CdSe-BA	CdSe-FBA
QDs Size (nm)	2.8 ± 0.1	4.0 ± 0.2	3.6 ± 0.2
QDs (μmole) / PMMA (g)	0.25	0.2	0.44

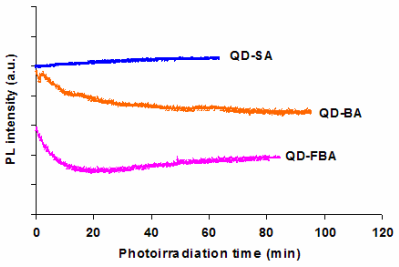

Fig. 2 (left) Peak PL vs. time for the QD – SA, BA and FBA films as monitored during the N_2 purged photocuring process.

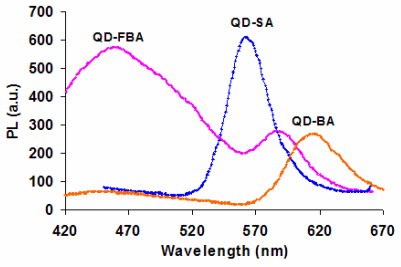

Fig. 3 (right) PL spectra taken after photoirradiation under N_2 for the QD – SA, BA and FBA films.

seen in previous studies. PL spectra collected after the photocuring (Fig. 3) resolve QD emissions at 562, 587 and 612 nm for unmodified QD-SA and surface modified QD-FBA and QD-BA films, respectively, while the broad peak at 458 nm with QD-FBA arises from excimers formed from [41] FBA group when FBA:TOPO reagent molar ratio was larger than 1:39. The observed QD emission peak intensity was monitored as a function of time for each of the films during the exposure experiments.

A representative reliability for the drop coating technique is presented in Figure 4 for QD-FBA films. PL spectra of 15 separate films show consistent peak position at 580 nm with a peak intensity variation of about 13%, and correspondently 250 ppm xylene sensing tracers for 5 of the 15 films display the sensing signal variation by 9%. These indicate that the drop coating technique allows the deposition of films with a reasonably reproducible PL and PL response properties.

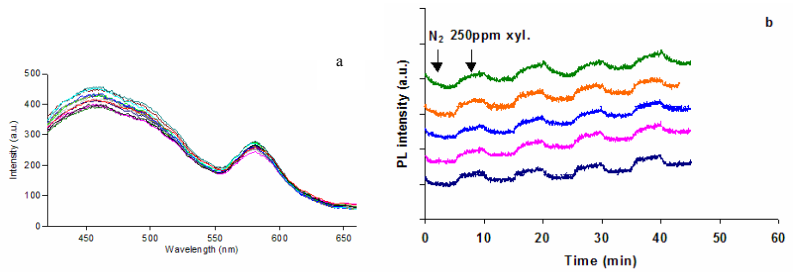

Fig. 4 (a) PL spectra of 15 drop coated QD-FBA films and (b) peak PL intensity responses of five of these films towards 250 ppm xylenes exposure

Fig. 5 displays peak PL intensity responses of QD-SA/PMMA system toward exposures of toluene and xylenes at concentrations below 1250 ppm, where the arrows are used to indicate the center of exposure (nitrogen or nitrogen/hydrocarbon) cycles. The observed PL baseline up-shifting may be ascribed to residual sticky HCs left in the film, which did not have enough time to get released within the 5-minute nitrogen cycle time. PL reversibly enhances upon exposure to low levels of HCs. Detection limits of 250 and ~500 ppm for xyelens and toluene were determined from the traces according to a definition of signal/noise ratio (S/N) of ~2. However, the PL intensity enhancement tends to decrease with a further increase in HC concentration, starting at ~1000 ppm for

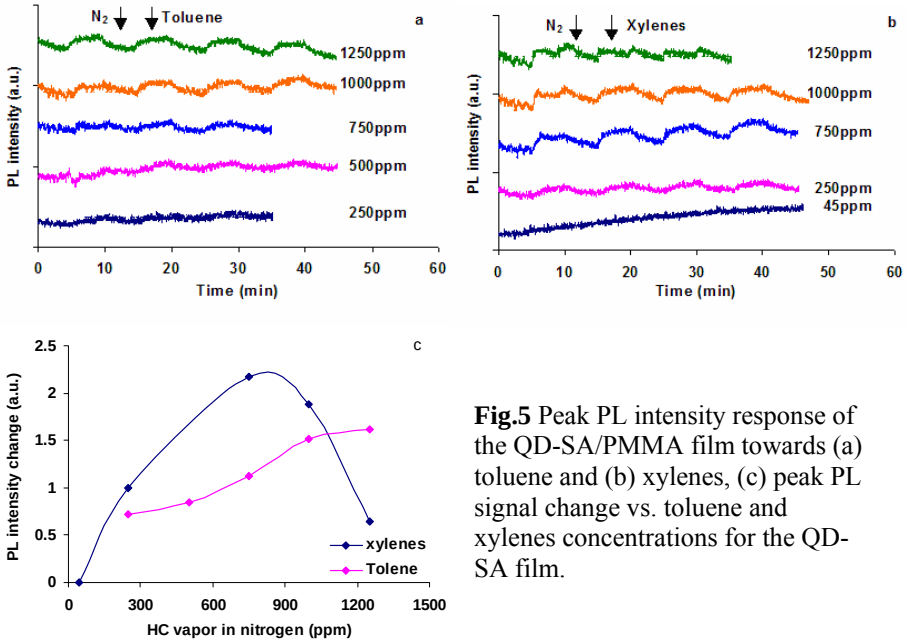

Fig.5 Peak PL intensity response of the QD-SA/PMMA film towards (a) toluene and (b) xylenes, (c) peak PL signal change vs. toluene and xylenes concentrations for the QD-SA film.

xylenes and ~1250 ppm for toluene, respectively, due to a competing PL quenching effect (see Fig. 6 below). The PL enhancement is believed to arise from improved passivation of non-radiative surface states of the QDs [42] in the presence of the electromagnetic field introduced by the surface interacted HC molecules [43]. The observed selectivity between xyelens and toluene, which differ by one methyl group, may illustrates that the methyl group have some donor property to QDs when the molecules approach to or become physisorbed onto the QD surface under photoirradiation. The sensing process seems depending on both the polarity and the electron donation strength of the target molecules and, therefore, permits a degree of selectivity for different chemicals, as evidenced here from the sensitivity difference between toluene and xylenes.

In contrast to the PL enhancement responses, when exposed to 2 % toluene and 0.94 % xylenes as an example, the QD-SA PL intensity displays a significant decrease, or PL quenching (Figure 6). This effect leads to non-monotonic sensing as shown in Fig. 5c, limiting the material for sensing application if not addressed.

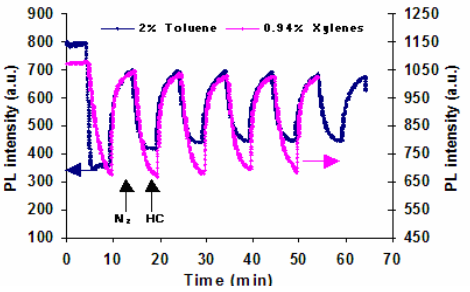

Fig. 6 PL intensity response of a QD-SA film toward exposure to 2 % toluene and 0.94 % xylenes in nitrogen.

Of particular interest is that introduction of BA or FBA onto QD surfaces indeed enhances sensitivity and selectivity of the QD based sensing materials. As presented in Fig. 7, the QD-FBA film clearly demonstrates PL responses to exposures of 15 ppm xylenes and 50 ppm toluene, a factor of 16 and 10 improvements in the detection limits towards xylenes and toluene, compared to QD-SA system. In addition, a selectivity factor of ~3 for the detection of xylenes over toluene is

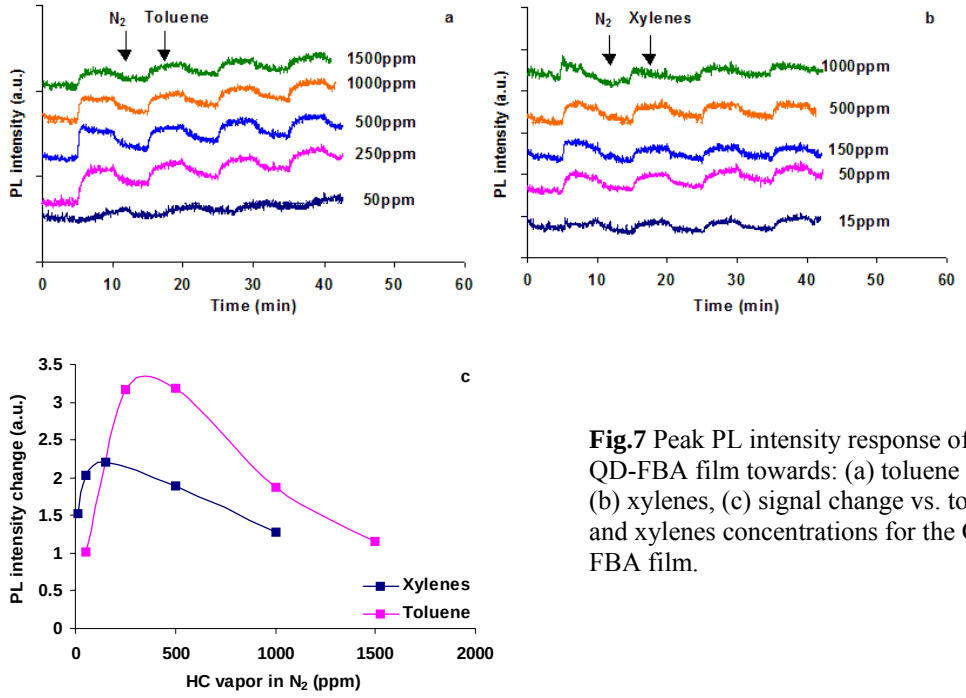

Fig.7 Peak PL intensity response of the QD-FBA film towards: (a) toluene and (b) xylenes, (c) signal change vs. toluene and xylenes concentrations for the QD-FBA film.

observed with QD-FBA. To our knowledge, both sensitivity and selectivity with our QD sensing materials are the best compared to what have been reported in the literature by other groups. This improvement confirms that introductions of BA or FBA as the electron-withdrawing "surface enhancing" groups onto the QD surface allow enhanced interactions between QDs and targeted analytes. However, again, for surface modified QD system, PL enhancement is competed by PL quenching during HC exposure process, resulting in undesired monotonic sensing (Fig. 7c).

A comparison of normalized sensing capabilities of QD-SA, QD-BA and QD-FBA films towards 50 ppm xylenes exposure clearly illustrate the role of the surface functional group (Fig. 8). The arylcarboxylate surface modified QDs show obvious sensing in contrast to non-sensing with unmodified QD-SA at this exposure. A factor of ~1.4 larger sensing signal with QD-FBA over QD-BA indicates that F-substituent to the π-system of benzoic acid likely proffers its electron-deficient properties and enhances the surface interaction of QDs with the targeted HC molecules.

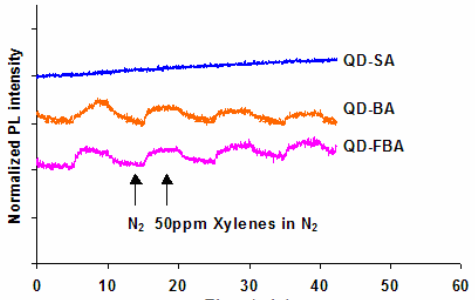

Fig.8 A comparison of the sensing capabilities of QD-SA, QD-BA and QD-FBA films towards exposure to 50 ppm xylenes.

While these results demonstrate promise for the development of sensitive and selective QD based hydrocarbon sensors, a close examination of the QD size, loading, and ligand coverage of these QD systems will provide further insight into the characteristics that account for the observed sensing enhancement. Detailed studies, which map out the sensing characteristics as a function of surface group type and coverage are presented below to provide a more complete understanding of the sensing mechanism of these surface modified QDs.

B. Effect of surface ligand type and coverage on hydrocarbon sensitivity and selectivity with CdSe Quantum Dots

In addition BA, FBA, we introduced naphthylamine (NA) as surface ligand to tune the QD surface chemistry by the synthesis method outlined above. This ligand has two aromatic rings and is expected to enhance pi-pi stacking interaction with HCs. Examining and analyzing the effect of the surface attached different groups and their coverage is the scheme of this reported work. Listed in Table 2 is the QD size and loading for each of the QD/PMMA films (NA1, 2, 3) and other samples for comparison. Fig. 9 is the structures of the ligand molecules used as surface

Table 2. Size, concentration and NA Surface Ligand Coverage on CdSe Quantum Dots

Sample	QD-NA1	QD-NA2	QD-NA3	CdSe-SA	CdSe-BA	CdSe-FBA
QD Diameter	2.8	3.0	3.0	2.8	4.0	3.6
µmol of QD/ g PMMA	0.30	0.15	0.09	0.25	0.2	0.44
mmol of NA	0.049	0.04	0.016			

reagents and a schematic diagram of potential interaction of the QD surface bound group, here FBA, with toluene and xylenes.

PL spectra of the various QDs/PMMA systems are presented in Fig 10, where for each of the curves the peak appearing at longer wavelengths, > 530 nm, is characteristic of the QD emission, while the broader peaks at lower wavelengths originate from excimers of the respective surface modifying groups. The surface group

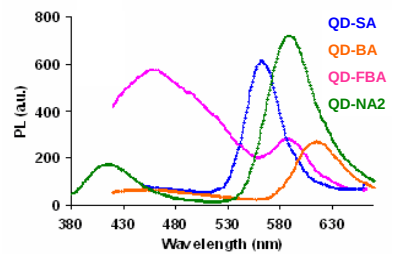

Fig.10 Fluorescence spectra of PMMA films with imbedded CdSe QDs with different surface groups: unmodified QD-SA, BA, FBA and NA surface modified CdSe QDs

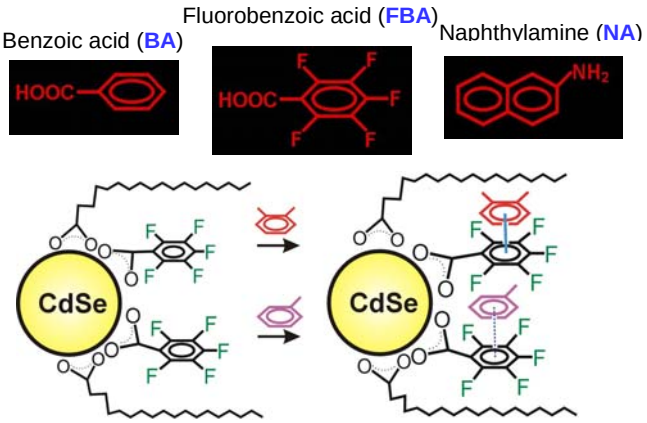

Fig. 9 Schematic representation of the QDs modified with surface enhancing reagents.

excimer forms with an increase in surface ligand coverage and an increase in QD loading in the polymer film. An overabundance of the excimer reduces the QD's absorption and emission and therefore it needs to be reduced to a certain level such that the QD emission is increased and hydrocarbon detection sensitivity is maximized, via adjustment of the surface group coverage, as discussed in detail below.

For comparison under the same experimental condition, the newly created QD-NA/polymer system was first tested with using N_2 as a carrier gas. Fig 11 compares the normalized sensing capabilities of the unmodified QD-SA films with the "surface modified" QD-BA, QD-FBA and QD-NA2 films, towards 50 ppm of xylenes in nitrogen. Though some differences in the QD size, QD loading and the coverage of the surface group (see Table 2 and excimer emission peaks in Fig. 10 may influence the sensing characteristics presented, they, however, are determined to be not main factors responsible for the observed sensing differences. It is thus clear again that the arylcarboxylate surface modified QDs have a higher sensitivity towards xylenes compared to that of the unmodified QD films, which show no measurable response at this concentration. There is an increase, a factor of 2.2, in the observed signal change towards xylenes for the QD-FBA film over that with the BA surface-bound group, which may be due to the more pronounced electron-withdrawing properties of FBA relative to that of BA. The QD-NA2 films also show an increased signal change of 1.2 over the QD-BA films, however the QD-

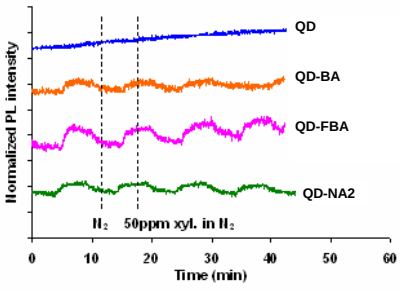

Fig. 11 Comparison of the sensitivity of the QD films towards a 50ppm xylenes in nitrogen exposure

FBA has a signal change, which is 1.8 times larger than the QD-NA2 response. These results indicate that the addition of the fluorinated aromatic ring systems to the surface-bound reagents increases most the sensitivity of the QD sensing response.

The selectivity characteristics of the QD-FBA and QD-NA2 films were challenged through the comparison of their response towards 50ppm xylenes and toluene exposures in nitrogen, as shown in Fig 12. For both QD systems exposure to the more electron donating xylene target molecule induces a larger response (by a factor of 2.5 for FBA and 1.8 for NA2) over the toluene exposure, thus displaying a degree of selectivity towards the detection of HC molecules that only differ by a single methyl group. The sensing process is consistently seen depending on both the polarity and the electron donation strength of the target molecules and, therefore, permits a degree of selectivity for different chemicals.

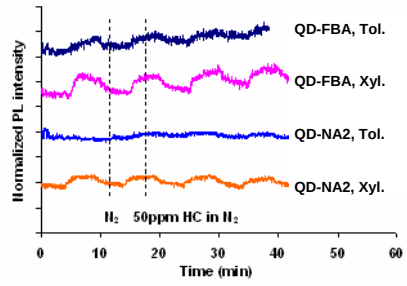

Fig. 12 Comparison of the selectivity of the QD films towards a 50ppm xylenes or 50ppm toluene in nitrogen

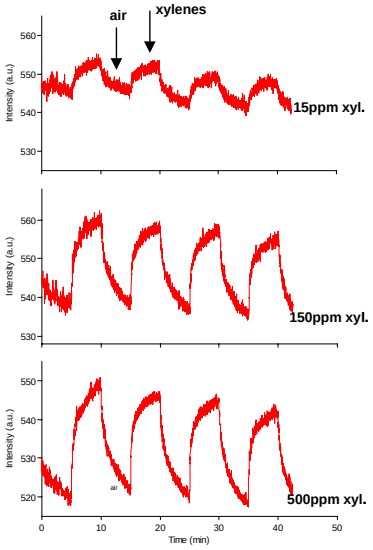

Fig. 13 Peak PL intensity change of QD-NA/PMMA film with chemical exposure time, with the exposure cycled between air and xylenes at different concentration levels

Apart from the sensing dependence on the type of the surface modifying groups, the coverage of the surface group may be also a factor influencing the sensing characteristics. Therefore, we further carried out a study on that with using QD-NA/PMMA systems of 3 NA coverage (Table 2) and more realistic dry air as carrier gas for testing. Displayed in Fig. 13 is a representative sensing performance towards exposure to low hydrocarbon concentrations in air for the QD-NA2 film. The peak PL intensity increases upon exposure to xylenes, and the PL enhancement increases with the exposed chemical concentrations. Very promising is that apart from the stable sensing performance in air, the sensing signal is large even at 15 ppm xylenes exposure (PL change by ~7.5 a.u.), inferring that the detection limit could be down to hundreds of ppb level.

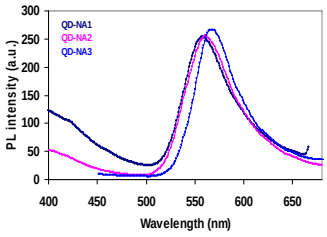

Fig. 14 PL comparison of QD-NA films made from QD-NA solutions with three different NA surface coverages

The surface coverage of 3 QD-NA samples synthesized with different molar contents of NA (Table 2) is qualitatively analyzed from a determination of the relative ratio of the PL intensity of the QDs to that of the surface group excimers. As seen in Fig 14 the peak intensity of QD emission (at wavelength > 550nm) is reasonably constant while that of NA excimer emission (at wavelength < 450 nm) is apparently different for the three QD-NA/PMMA films. Though the NA excimer PL peaks were not

fully collected for all the 3 samples, it is readily apparent from Fig 14 that the excimer peak PL intensity is reduced in accordance with the reduction in the NA reagent molar content for the NA3, NA2 and NA1 films. Furthermore, it is a reasonable assumption that the NA surface coverage should decrease with the decreasing NA quantities used in the synthesis process. The sensing traces of the 3 QD-NA samples in Fig 15 show a maximum signal change at a medium surface coverage (NA2), while too little or too much NA coverage leads to weaker sensing responses. For the QD-NA3 sample this is most likely due to a lack of surface species available for interaction with the target molecules, while the reduced signal change observed at a high surface coverage (NA1) is likely due to the formation NA excimers which modify the interaction capabilities of the surface groups with the target molecule. It appears from these initial studies that a balance between having enough NA species available for interaction enahncing while not inducing a large quantity of excimer formation can provide a sensing film with an enhanced sensitivity towards hydrocarbon detection.

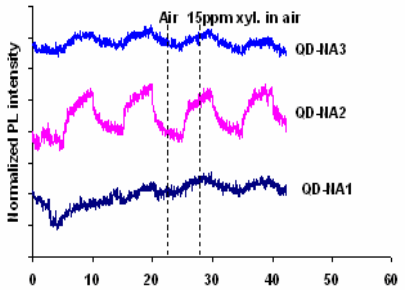

Fig. 15 Comparison of QD-NA sensing characteristics as a function of NA coverage

From the above qualitative arguments it is clear that the sensing characteristics are dependent on both the surface modifying group type and its corresponding surface coverage.

C. Synthesis of nanocomposite materials with controlled structures and optical emissions: application of various methacrylate polymers for CdSe quantum dots encapsulation

As a second level for development QD based sensing materials, we investigated in different methods for constructing CdSe QDs into macroscopic element for the sensing study. Here, CdSe Quantum Dots (QD) were incorporated in polymer films via in situ polymerization using one of four different monomers having a varied hydrocarbon side chain length, namely hexyl, lauryl, stearyl, or behenyl methacrylate. Fig. 16 is a schematic representation of CdSe QDs dispersion in poly(hexyl methacrylate) by in situ polymerization, while displayed in Fig. 17 are photos of the CdSe QDs in polymers with side chain lengths of : a) C_{18}, b) C_{12}.

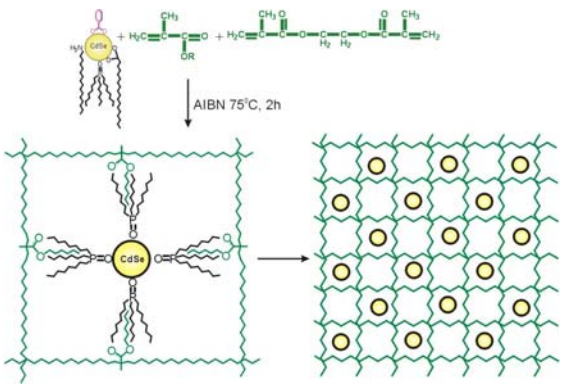

Fig. 16 Schematic representation of CdSe QDs dispersion in poly(hexyl methacrylate) after in situ polymerization. Monomers: hexyl methacrylate: -R is $-C_6H_{13}$, lauryl methacrylate: -R is $–C_{12}H_{25}$, stearyl methacrylate: -R is $–C_{18}H_{37}$ and behenyl methacrylate: -R is $–C_{22}H_{45}$.

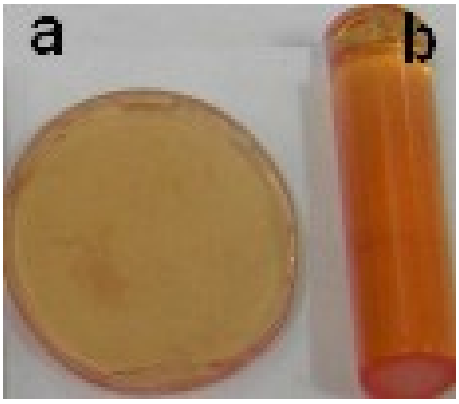

Fig. 17: Photos of the CdSe in polymers: a) C_{18}, b) C_{12}.

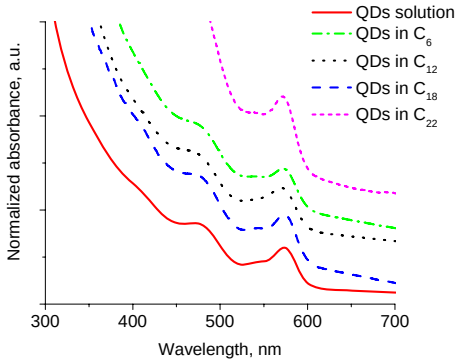

Fig. 18: UV-vis absorption spectra of QDs in polymers

Importantly, the UV-vis absorption spectra of the four types of polymer films with embedded 4 nm QDs all demonstrate non-broadened characteristic first excitonic peak at 586 nm, analogous to that of 4 nm QDs in chloroform (Fig. 18). This is appealing since broadening and red-shifting of the QD absorbance bands means a transition from isolated QDs, with localized electronic states, to the delocalized electron-hole states characteristic of QD clusters, i.e. of close-packed ensembles of QDs. Thus our results may imply a low degree of particle aggregation during in-situ polymerization in our samples. As confirmed, laser scanning confocal microscopy images (Fig. 19) shows a relatively homogeneous and non-long-range ordered distribution of QDs along with some QD clusters within the randomized polymer matrices.

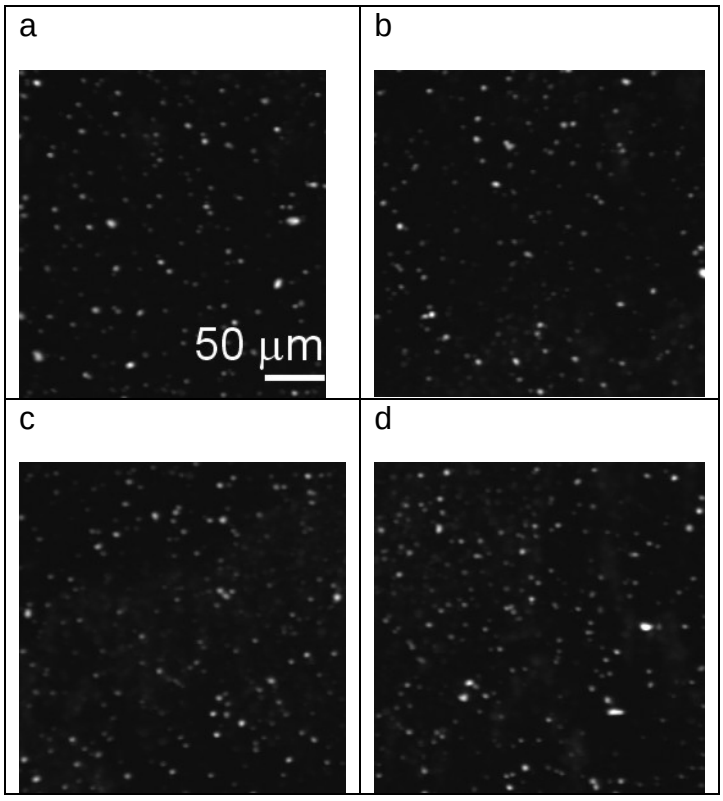

Fig. 19: Confocal microscopic images of CdSe/polymer films. a) C_6, b) C_{12}, c) C_{18} and d) C_{22}

The fluorescence spectra of the QDs in a chloroform solution and in polymer matrices present nearly identical emission spectra, indicating that no significant increase in particle

size has occurred during the polymerization process (Fig. 20). The thickness of all nanocomposite QD/polymer films used for the PL measurements was controlled within 1 mm. Fig. 21 details the PL measurements for 9 different points of the same CdSe/C_{12} film. The PL peak intensity variation at 586 nm is about 23%, which may be related to the variation in local thickness of the films.

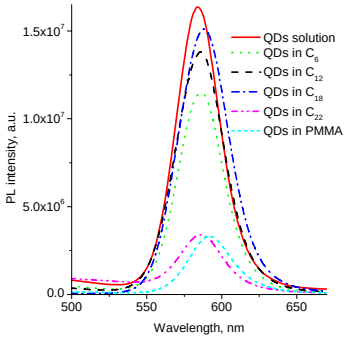

Fig. 20: Photoluminescence spectra of QDs in polymers

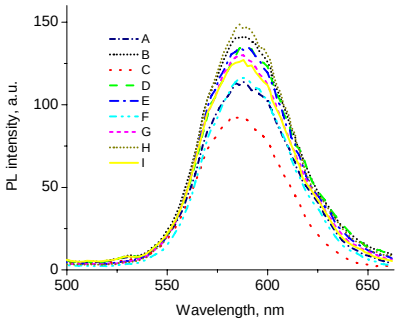

Fig. 21: PL spectra of 9 different points of the same CdSe/C_{12} film

From the fluorescence quantum yields (QY) of 1 mm thick QD/polymer films listed in Table 3, it is noteworthy that the QYs of QDs in polymer matrices with C_6 and C_{22} branches are quite low while that with C_{12} is almost as high as the initial QY of the QDs in a diluted solution. This is probably due to a reason that C_6 and C_{22} branches of hexylmethacrylate and behenylmethacrylate are too short or too long to allow QDs to be optimally packed in the cages (see Fig. 1) formed during polymerization, leading to QD aggregation and PL quenching; instead moderate long alkyl branch monomer C_{12} or didecyldimethlylammonium methacrylate prevents QD from aggregating inside polymers and thus avoids PL quenching.

Table 3: PL quantum yields (QY) of QDs in hexane solution and in thin polymer matrixes

Sample	**QDs in solution**	**QD, C_6**	**QD, C_{12}**	**QD, C_{18}**	**QD,C_{22}**
QY (%), before photocuring	37.1	7.9	32.1	24.8	0.8
QY (%), after photocuring	8.2±0.9	6.6±0.9	2.5±0.1	3.1±0.1	19.5±0.3

Photocuring of the co-polymerized QDs/polymer films under 350-nm light illumination and air ambient leads to their QY increase except a slight QY decrease with C_{12} (Table 3). This is consistent with the literature reported increase in QY for photo-curred QDs in the case of poly(dimethyl siloxane) and poly(butadiene). This photoactivation probably results from passivation of the QD surface through removal of surface traps and system relaxation. Compared in Fig. 22 are PL spectra of QDs in C_{12} polymer before and after 20 hours of photocurring, revealing no photo-degradation induced PL blue shift, which is a

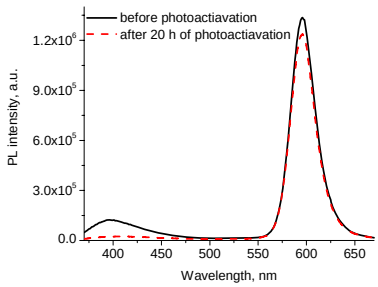

Fig. 22 PL changes before and after of 20 hours of photoactivation at 350 nm irradiation of QDs in C_{12}

common instability issue with QDs in solution or films. The PL spectra of QDs in other polymer systems, C_6, C_{18} and C_{22}, also do not reveal any undesired blue shift after photocuring.

Following the in-situ polymerization of methacrylate monomers with QDs to make nanocomposite films, we conducted xylenes sensing test for QD-NA/polymer with C_{12} and obtained the result shown in Fig. 23. However, as one can see, the samples show no sensing toward 1000 ppm xylenes exposure, which is in significant contrast to 15 ppm or lower detection limit achieved with drop coating technique prepared QDs/PMMA film as presented previously. Thus, the presence of long polymeric chains seems beneficial for an even dispersion of QDs in polymethacrylate matrices with retaining of QDs optical properties, but this encapsulation of QDs results in a drastic decrease of their sensing properties toward aromatic hydrocarbons. Moreover, no improvement of the surface-modified QDs (by e.g., FBA) sensing properties was observed for the embedded polymer films, possibly indicating that the QDs were well encapsulated during the in-situ polymerization, thus leading to limited QD surface interactions with its surrounding environment.

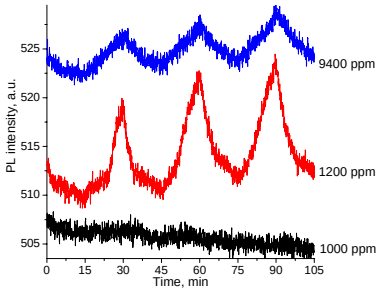

Fig. 23 PL intensity changes of QDs-NA 10wt% in C_{12} while exposure to xylenes

D. Fabrication of highly-ordered luminescent multilayered thin films of CdSe quantum Dots

We then explore controlled integration of functionally distinct QDs into uniform 2D and 3D nanoparticle-based layers. This consists of in-situ surface functionalization of CdSe QDs in synthesis process and then layer-by-layer immobilization of the QDs on solid substrates by means of solution-immersed self-assembly via surface modification of a substrate with functional groups that provide attractive interactions with the surface functional group of the deposited nanoparticles.

As a key step to this approach, we have successfully functionalized the QDs surface with 11-hydroxyundecanoic acid (11-HUDA) during in-situ preparation to afford stable and highly luminescent quantum dot solutions (see Fig.24). The novelty of this developed technique is that it avoids using common ligand exchange processes that could otherwise lead to a significant loss in PL, a general problem suffered, since as shown in this figure, the narrow (the full width at half-

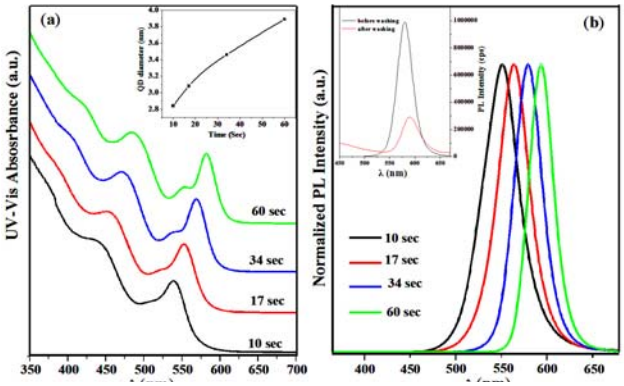

Fig. 24 The optical absorbance (a) and PL (b) spectra of the in situ functionalized CdSe QDs collected at different time intervals. The insets show (a) the calculated QDs diameter vs. time of collection and (b) the PL properties of the QDs before and after washing.

maximum, fwhm, is ~ 25-40 nm) and strong photoluminescence of the quantum dots confirm that the in-situ addition of 11-HUDA does not hamper the optical properties of the resulting QDs. The QD diameter (inset in Fig. 1a), determined from the first absorbance peak, increases with processing time, and correspondently, both the absorption band edge (first peak) and PL shifts to longer wavelength. The QDs were purified with washing prior to their use, and a comparison of the PL intensity of the QDs before and after washings is shown in the inset in Fig. 24b.

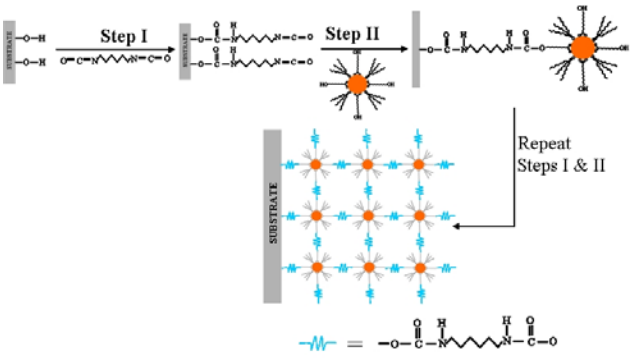

Fig. 25 Schematic illustration of functionalization of a glass substrate by HMDIC followed by immobilization of the 11-HUDA surface-modified CdSe nanoparticles on the isocyanate-bearing substrate through the carbamate-bond forming reaction.

Next, the monolayer formation approach is based on the covalent bond forming reactions between 11-HUDA grafted on the surface of CdSe QDs and the 1,6-hexamethylene diisocyanate (HMDIC) molecules that serves as an organic linker between QDs and to a glass substrate (pretreated with alkaline solution resulting in a hydrophilic surface). These reactions facilitate the immobilization of nanoparticles onto solid supports and allow the construction of three-dimensional networks of QDs in a layer-by-layer fashion as detailed in Fig. 25 for the coupling scheme. Importantly, the carbamate bond formed between the CdSe QDs and the substrate prevents the CdSe nanoparticles from being removed by, for example, repeated washings with several organic solvents and water at a wide range of pH under ultrasonication.

3.5 nm sized QDs were used for a successive layer-by-layer fabrication to make desired thickness (1 to 12 layers) by repeating the above steps with each layer of QDs being covalently bonded and separated by a fixed distance designated by the organic linker. Plots of the first absorbance peak intensity of the QDs *vs* number of layers (on glass substrate) are linear through the origin (inset in Fig. 26a, indicating that the deposition of the QDs was uniform in each step during the film formation process, i.e., equal amounts of nanoparticles have been deposited in each cycle of fabrication. The PL spectra of the same films (Fig. 26b) also indicate a gradual increase in the PL intensity with the successive

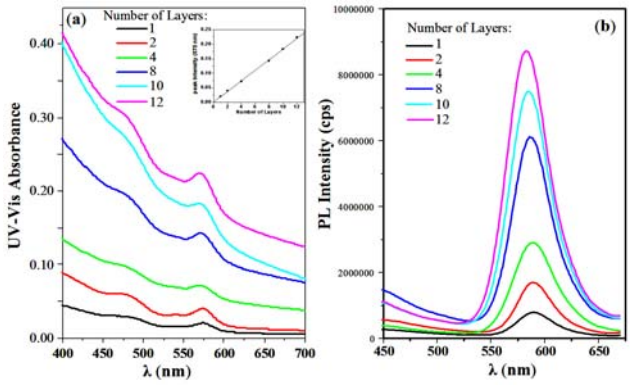

Fig. 26 (a) Optical absorbance spectra of the multilayered films. Inset represents the linear-fitting curve for the peak at 570 nm as a function of the number of deposited layers on a glass substrate. (b) PL spectra of the corresponding films.

increase in the number of layers. The QY of the 12 layered QDs film was estimated to be 6 %.

Further more, bright field TEM photograph of the 11-HUDA functionalized CdSe QDs after washing (Fig. 27a) confirms that the particles are nearly monodisperse without particle aggregates and the measured particle size of ~3.7 nm is in good agreement with the optical absorbance calculations. The AFM image (Fig. 27c) provides an evidence of a

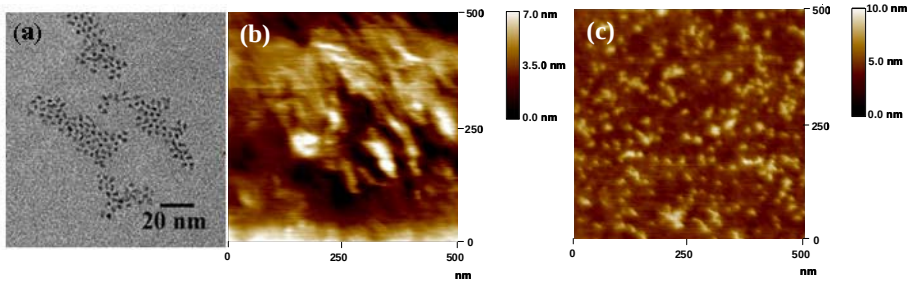

Fig. 27. The bright field TEM image of the 11-HUDA functionalized CdSe QDs after washing; The AFM images of the isocyanate-bearing glass substrate (b), a monolayer of CdSe QDs on a glass (c).

roughly monolyaer of immobilized CdSe QDs on a glass in comparison to non-particle AFM image (Fig. 27b) of the isocyanate-bearing glass substrate. AFM height profile in several regions of this film yielded only a 3.7 nm difference between the highest and lowest points, correspondent to the estimated thickness of the QD monolayer. The observed slightly different packing of the immobilized CdSe nanoparticles than expected dense and ordered pack is presumably due, in part, to the inhomogeneous distribution of the first isocyanate functionality on the glass substrate (Fig. 27b).

The separation distance between QDs can be adjusted with using longer chain hydroxycarboxylic acids, such as (16-HHDA), to link to HMDIC. Similarly, the optical absorbance and PL spectra of such prepared QDs multilayered films with (16-HHDA) both present gradual increases upon increasing the number of layers (Fig. 28a). Impressive is that the resulting bright orange film shows no visible defects, opaque areas or color inhomogeneities (Fig. 28b). The films are robust and environmentally stable since there is no drastic change in the optical properties or oxidation observed after kept in air for weeks. The immobilized CdSe QDs on glass preserve QD absorbance in solution without peak shifting often seen

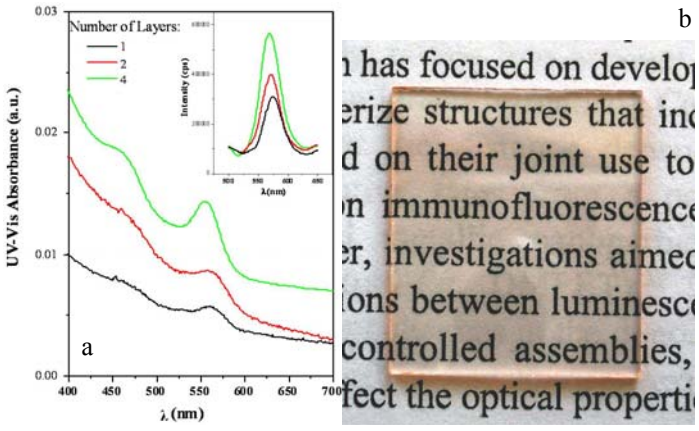

Fig. 28 (a) Optical absorbance spectra of the multilayered films fabricated using the 16-HHDA functionalized QDs with the inset showing the PL spectra of these films. (b) Photo of the 10 layered film fabricated on a glass slide.

with transferring QDs from solution to solid states. The observed slight blue shift (~7 nm) of PL peak position of the 12 layered QD film may be due to some oxidation of QDs during long multilayer build-up processes.

For assembling multiple layers of QDs on widely used silicon wafers, we chose 3-aminopropyltriethoxysilane(APTES) to chemically form dense self-assembled monolayers on native SiO_2 of silicon wafer for subsequent coupling with CdSe QDs. The Si surface-bound aminopropyl groups were covalently bound to HMDIC first, and the latter served as a linker reacting with 11-HUDA grafted on the CdSe QDs surfaces in order to make the covalently-bound layers, as shown in Fig. 29. The optical absorbance and PL intensity of the resulting Si-supported QD multilayered films increases monotonically with an increase in the number of layers (Fig. 30). The use of APTES as a Si-coupling agent improves the QDs attachment to the silicon wafer, since PL intensity in this case is substantially increased as compared to the non-APTES treated substrates (Fig. 30b).

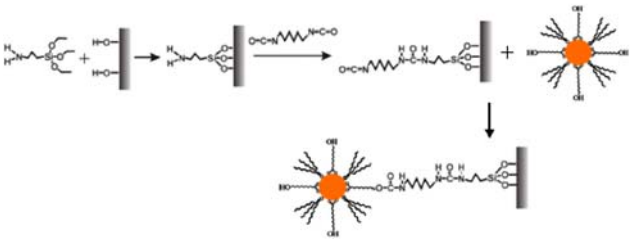

Fig. 29. Schematic illustration of functionalization of the silanized Si surface with hexamethylene diisocyanate followed by the immobilization of the surface-modified CdSe QD through a carbamate-bond forming reaction.

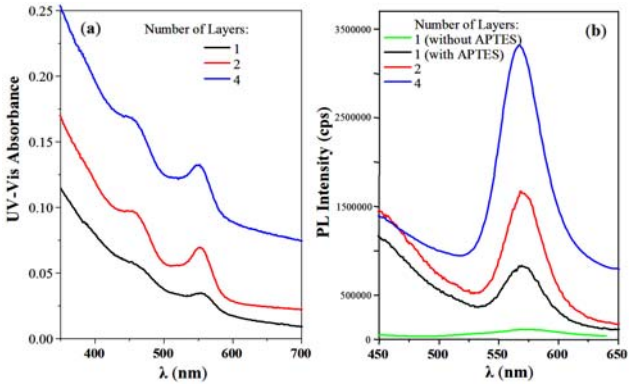

Fig. 30. (a) Optical absorbance and (b) PL spectra of the multilayered films fabricated on Si substrates.

It is noteworthy that the constructed multilayers of CdSe QDs on glass and Si substrates have long-term stability. No significant changes in optical absorbance and photoluminescence properties of these films were observed over 3 months period (Fig. 31). There is a small gradual blue shift in the emission of the QDs observed with time, which may be due to the gradual surface oxidation of the QDs with atmospheric oxygen. This contrasts the general observation of a red shift in most cases, illustrating that in our layer-by-layer grown films the capping effect of the functional groups prevents the agglomeration of the QDs.

Hydrocarbon exposure test of a 20 layer film of 11-HUDA bound QDs on a glass substrate demonstrates a sensing to 150 ppm xylenes but also exhibits undesired PL quenching and desensitization with an increase in the analyte

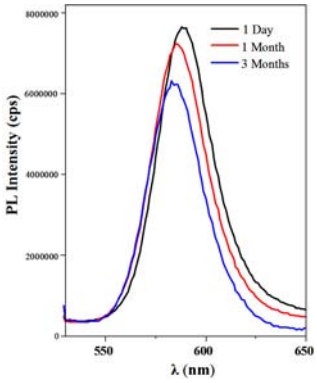

Fig. 31. PL intensity of the 10 layered CdSe-film on glass at different time

concentration. In spite of this non-promising performance as a sensor, this technique should be useful for the development of other QD-based optical and electronic devices that can harness the highly photoluminescent properties of these ordered and stable nanocomposite materials.

E. Sensing mechanism investigation: PL enhancement, PL quenching, inversion, desensitization

Different research groups have reported opposite PL responses (i.e., PL enhancement and quenching or decrease) for similar CdSe QDs systems toward exposure of similar analytes. We have also observed the same puzzle PL responses. The competition of the two effects leads to sensing signal inversion and desensitization and monotonic indication, limiting the practical study and application of these sensing materials. In this work, we present a study on the fabrication and sensing of CdSe/polymer nanocomposite films, aiming at understanding the mechanism behind and help address the mentioned obstacle.

So far, our research has demonstrated that drop casting technique seems the most appropriate method for building up QD sensing materials. However, proper and controlled preparation of QD/polymer thin films is still an important step toward developing operational sensors for specified sensing applications. Fig. 32a demonstrates ~270% higher PL intensity at a common peak position of ~587 nm for a CdSe-NA QD/PMMA film fabricated from a solution mixture of QDs/CF (chloroform) with PMMA/CB (chlorobenzene) (A) than that of a film fabricated from a mixture of QDs/CF with PMMA/CF (B) using the same QD/PMMA loading ratio for both. This is consistent with the much brighter red color of the optical microscopy (OM) image of sample A (Fig. 32b) since there is a significant contribution of QD's emission to the image color and intensity. The difference observed is attributed to a higher degree of roughness with sample A over sample B, as indicated by their OM images and also visual appearance. The rougher surface induces more scattering effect that enhances optical absorption and emission for sample A. Slight immiscibility of chloroform and chlorobenzene in the solution mixture is believed to contribute to the rougher feature formation of sample A.

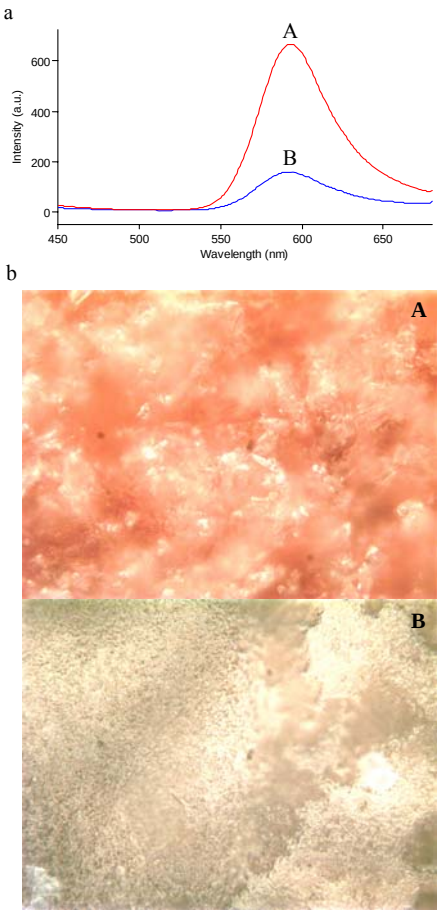

Fig.32 Comparison of (a) photoluminescence and (b) Optical Microscope images of CdSe quantum dot/PMMA thin films having different surface roughness, sample A and B

As a result, sample A displays nice PL enhancement responses upon exposure to low levels (< ~ 1000ppm) of xylenes with

detection limit of ~ 15 ppm (Fig. 33a), while sample B shows unobservable PL enhancement at 50ppm xylenes, followed by PL quenching at increased xylenes levels (Fig. 34). These results are repeatable and suggest that rough nanostructured QD/polymer films are preferred over smooth and clear films for QD-based gas sensing. Thus, in the following sections, only samples fabricated with method A are the subjects of further investigation and discussion.

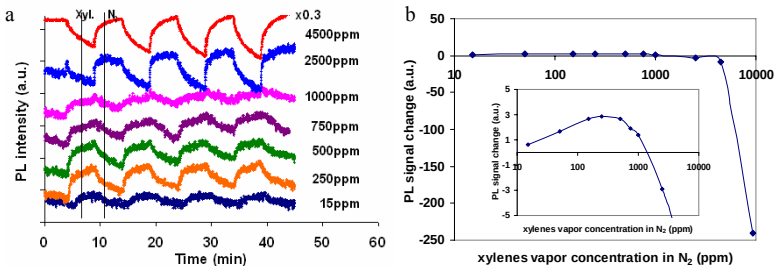

Fig.33 (a) PL peak intensity responses to exposures of xylenes at different concentrations and (b) the sensing characteristics as a function of xylenes concentration, from a CdSe quantum dot/PMMA thin film prepared with method A described in the text, where the inset in (b) shows the detail at low hydrocarbon level exposures.

The PL enhancement of sample A reaches a maximum at ~280 ppm xylenes (inversion point), followed by a decrease to zero at ~ 1000 ppm xylenes (desensitization point) and then by a significant PL quenching with a further increase in xylenes concentration to 9400 ppm (Fig. 33b). This non-monotonic sensing is typical of these QD/PMMA films toward HCs species and other chemicals, e.g. methanol (not shown here).

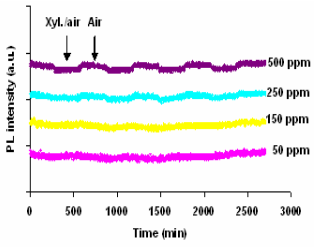

Fig. 34 PL peak intensity responses to exposures of xylenes at different concentrations from a CdSe quantum dot/PMMA thin film prepared with method B described in the text

For elucidating the observed sensing characteristics we performed counterpart experiments on QD solutions exposed to a variable amount of liquid xylenes. To do so, we mixed 20µl of $4.6x10^{-6}$ mol/l CdSe-NA QDs in $CHCl_3$ with a volume of xylenes (0, 20, 40, 60 or 80 µl) using $CHCl_3$ as a buffer so that the total solution volume was held constant at 100µl. As shown in Fig. 35, the PL intensity monotonically increases until the xylenes volume reaches ~40µl, while the absorbance remains the same for all of the solutions. A similar trend with xylenes is observed for QD solutions in the co-presence of PMMA (Fig. 35b). The consistent PL enhancement seen for the QD solutions upon xylenes addition illustrates an intrinsic interaction between the colloidal QDs and analytes since there is no other factor that may cause the PL response in the solution phase. Therefore, the PL enhancement observed from the QD/PMMA films during the HC sensing process should also originate from the interaction of the

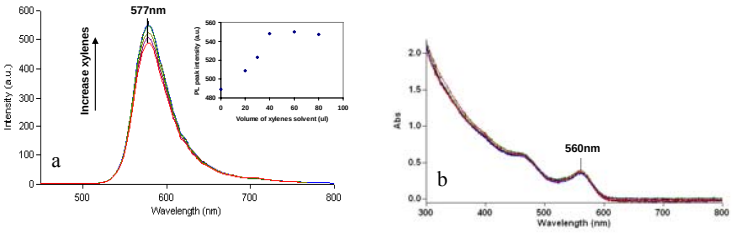

Fig. 35 (a) Photoluminescence and (b) absorbance of solution samples of CdSe-NA QDs in $CHCl_3$ mixed with different volumes of liquid xylenes, where the inset in (a) shows peak PL intensity as a function of xylenes volume.

QDs with analytes, which is thought to enhance passivation of surface states of the QDs and reduces photo-generated electron-hole recombination rate in the local electrical field brought in by the analyte. There, the hydrocarbon molecules seem to serve as a Lewis base, donating electrons to the QDs studied in this work.

Competed by PL quenching, PL enhancement of CdSe QD/polymer starts to decrease (inversion) with an increase in HC concentration. The inversion point varies from QD/polymer film to film, depending on a combined attraction ability of the surface-modified QDs and the polymer hosts toward HC species and thus the amount of HC absorbed in the film. As shown in Fig 36a, for the same xylenes species, the inversion point shifts from ~800, to 280 and 150 ppm xylenes for unmodified and NA and FBA surface modified QDs, respectively, corresponding to the decreasing trend in their HC detection limits, while in Fig. 36b, for the same CdSe-FBA QDs, exposure to xylenes causes a lower inversion point (150 ppm) with regard to 250 ppm for toluene exposure due likely to the reason that xylenes are more prone to be absorbed in the film with its one more methyl group enhanced interactivity. An increase in QD loading in the polymer host leads to a shift of the inversion point to lower HC concentrations owing to an increased absorption of HCs in the film in the presence of greater amounts of QDs. The polymer matrix used also plays a role in affecting the PL quenching and the inversion behavior, as the polymer itself has a characteristic chemical affinity and solubility toward the various target chemicals.

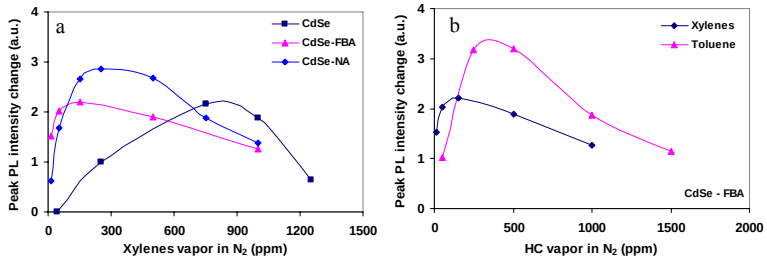

Fig.36 Sensing signal of peak PL intensity change of QD/PMMA films as a function of HC vapor concentration in N_2 for (a) different surface modifying groups bound to CdSe QDs, (b) different types of targeted hydrocarbon species exposed to the same CdSe-FBA QDs

A key observation for understanding PL quenching is that a QD/PMMA film kept in a covered dish saturated with HC vapor pressure showed an apparent wetting appearance. This initiated our experiment to monitor absorbance and fluorescence change from the film under cyclic exposure to N_2 and high level HC in N_2. The plot in Fig. 37a shows that upon exposure of a CdSe-NA QD/PMMA film to 9400ppm xylenes, the absorbance reversibly drops dramatically in the whole band, which explains why there is a

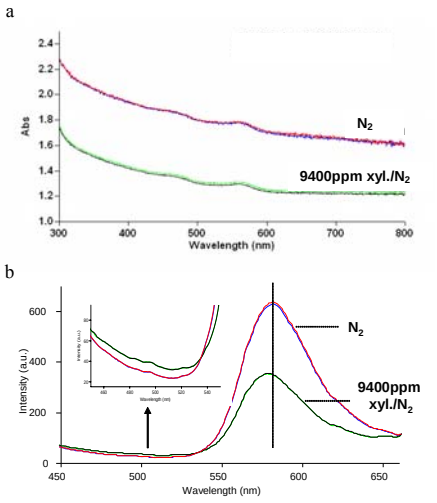

Fig.37 Two-cycle reversible change in (a) absorbance of CdSe-NA substrate and (b) photoluminescence of CdSe-NA QD/PMMM film on a silicon substrate, QD/PMMM film on a glass under exposures switched between N_2 and 9400 ppm xylenes mixed with N_2, where the inset in (b) shows a background signal change

huge PL quenching from a similar film coated on silicon (the PL reduction effect is irrespective of using glass or silicon substrates) since less light is absorbed by the QDs. This reduced absorption and emission by QDs supports that the film gets wet and clear (refractive index changed) when a high amount xylenes vapor is absorbed in the film. In addition, the reversible PL peak blue shift and baseline increase (blow 550 nm) under the xylenes exposure (Fig. 37b) verifies the wetting and clearing effect since the detector captured more stray light due to more reflection of incident light from the Si substrate covered with the clearing film. Further, this effect is evidenced with the fluorescence image of the film exposed to 9400 ppm xylenes (Fig. 38a) compared to the bright images (camera capture time is even 4 time shorter) of the film in N_2 (Fig. 38b) and reversible formation of xylenes-bubble like features on the image center (Fig. 38b). Experimentally, it has been observed that the wetting starts locally on the film surface at low levels of vapor HC concentration and evolves to a large area covering the film surface at high levels of HCs.

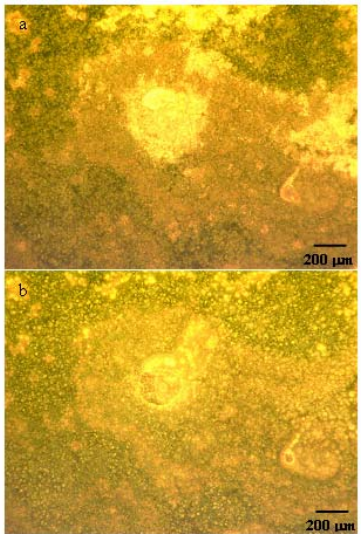

Fig.38 Reversible change of Fluorescence Optical Microscope images of a CdSe-NA QD/PMMA film exposed to (a) dry air and (b) 9400 ppm xylenes mixed with air. The CCD exposure time is 4 times shorter for image (a) than that for image (b).

Thus, the PL quenching is identified to result from increased HC vapor absorption induced wetting effect and resultant light/matter interaction change, including scattering, absorption, transmission, refractive index change. In this process, we speculate that there is a hydrocarbon wetting associated filling and smoothing effect taking place, which reduces the QD/polymer surface roughness enhanced scattering or local electromagnetic field, leading to attenuated light absorption and emission by the QDs. The wetting induced clearing effect reflects a modification of the refractive index of the QD/PMMA film due to absorption of external analyte, along with a possible formation of an analyte liquid layer during the HC exposure process, thus reducing the incident light absorption by QDs. These explanations were verified by the observation that the color and intensity of fluorescence images were immediately recovered upon removal of xylenes, as revealed by time-resolved OM imaging. The effect is likely extendable to different QD/polymer systems and other inorganic/organic hybrid systems. It is believed that the complexity of the sensing process with nanoparticle sensing material is revealed for first time. Addressing this effect through continued studies is critical for further development of QD based hydrocarbon sensors.

F. Dependence of hydrocarbon sensitivity on the separation distance of CdSe QD to the aromatic group of carrying liagnds attached to the QD surface

New sensing material fabricated by the technique we developed (detailed in next section) to integrate colloidal CdSe QDs on quasi photonic crystal (PC) anodic aluminum oxide (AAO) platform enables monotonic PL response to HC exposures over three orders of magnitude. Based on this new sample structure, we conducted a study on the

hydrocarbon sensing properties of CdSe QDs tailored with phenyl group carrying surface enhancement agents to determine the sensing dependence on the aromatic group distance from the QD surface. This work is expected to help develop a better understanding of the underlying sensing mechanisms along with methods for achieving the desired sensitivity, selectivity and reliability of QD-based chemical sensors.[36]

Fig. 39 shows similar UV-Vis absorbance spectra of four solutions of CdSe QDs capped with TOPO, SA and HDA as stabilizing agents but different acids as surface enhancement agents, namely, benzoic, phenylacetic, phenylbutanoic or phenylhexanoic acids (BA, PA, PBA, PHA). According to the data (see Table 4) calculated from Fig. 39, the QDs in the four solutions have close sizes, extinction coefficients, and concentrations, which is important for sensing comparison in this study, although there are slight increases in these values with changing the surface group from BA to PHA. Unexpected is that PL from QDs bound with PHA or PBA is much stronger than that with PA and BA (Fig. 40), which is in good agreement with the measured quantum yields (QY) listed in Table 4. The proportional correlation of quantum yield or PL with an increasing distance between the phenyl ring of the surface enhancing ligand and the QD surface may be an indication of charge transfer effect between them as detailed below.

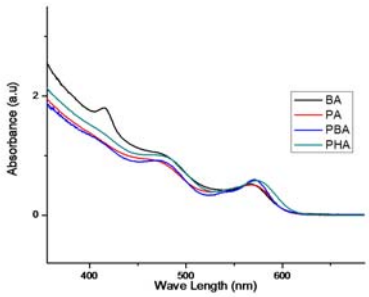

Fig.39. The absorbance spectra of CdSe QD solutions with same QD size and concentration.

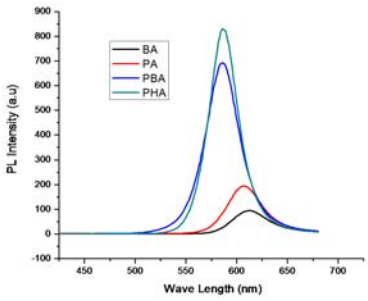

Fig.40. The photoluminescence spectra of CdSe QD solutions in chloroform with same QD size

Table 4. QD Size (nm), Extinction Coefficient ($cm^{-1}.M^{-1}$), Quantum Yield and QD solution molar

Sample	QD Size (nm)	Extinction Coefficient ($cm^{-1}.M^{-1}$)	QD Concentration (M)	Quantum Yield (%)
BA	3.4	154166	5.1E-06	4.5
PA	3.5	160676	4.7E-06	10.6
PBA	3.5	167574	4.8E-06	28.3
PHA	3.6	178705	4.9E-06	29.4

For this study, it is important to identify the surface coverages of the above surface bound agents to make sure they have similar values as different coverages will likely affect the degree of ligand to QD charge transfer effects. NMR is a powerful technique and capable foe this analysis. As an example, Fig. 41 reveals chemical shift and broadening of ^{1}HNMR spectra QD-bound PA

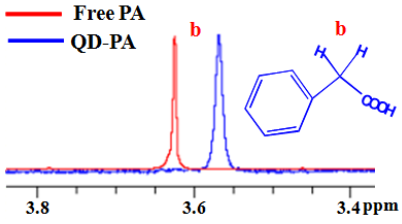

Fig. 41 Comparison of the singlet peak (b) in ^{1}H NMR spectra of free PA vs. bound PA to surface of QD.

ligands in chloroform compared to free PA in chloroform, proving that PA is indeed bound to the QD surface. Based on integration analysis of the NMR peaks for the nanoparticle samples, surface ligand molar values normalized to the surface-enhancing agent together with the normalized chemical reagent information used for the nanoparticle syntheses is given in Table 5. Moreover, by mixing the same amount of each QD (BA, PBA and PHA) separately with a QD-PA sample, the exact enhancing ligand ratios relative to PA were measured as 0.93, 0.95, and 1.13 for BA, PBA and PHA, respectively. Through this integration it can be seen that the ratio of surface enhancing

Table 5. Normalized mole ratios of various surface ligands of CdSe QDs with respect to surface enhancing agent determined by ^{1}HNMR along with synthesis values

Sample	Ligand	HDA	SA	TOPSe	TOPO
BA	1	15.4	NA	9.5	25.5
PA	1	13	5.5	9	23
PBA	1	14	NA	9	23
PHA	1	13	5	8.5	23
synthesis	1	15.5	4	10	21.2

ligand to the surface stabilizing ligands is essentially the same for the QD-BA, -PA, -PBA and -PHA samples, which is consistent with quite similar values expected from the reagent synthesis information. Moreover, since the ligand ratios of the QD-BA, -PBA and -PHA samples with respect to the QD -PA sample, are all approximately equal to 1, we can conclude that each of the QD samples used in this study have very similar ligand coverages, which is a critical point to verify prior to studying the hydrocarbon sensing results.

Thus, according to the studies presented in the literature, the cause of the observed decrease in quantum yield as a function of the phenyl ring to QD surface distance may result from charge transfer between the surface agent and the CdSe QD when they have similar surface coverage. The charge transfer seems more efficient for smaller BA bound QDs relative to the other surface enhancing ligands modified QDs. Therefore, it is not unexpected that when the aromatic ring gets further away from the QD surface in PBA and PHA ligand the quenching effect decreases and the PL intensity increases drastically. Other possible explanation for the lower quantum yield observed for the smaller ligand bound QD samples may pertain to possible accelerated growth

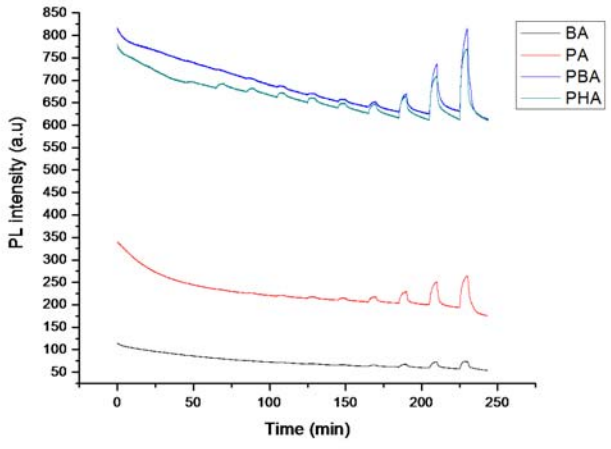

Fig.42 Gas on/off curves for four QD films on AAO substrate upon exposure to various concentrations of xylenes.

of particles. Also it could be associated with the ligand length itself and its overall affect on surface passivation.

Four QD films cast on AAO supports from the four solutions show consistent PL spectra pattern with that presented in Fig. 40 for QD solutions. Their sensing traces depicted in Fig.42 demonstrate PL enhancements upon exposure to xylenes in air over all the concentration range without PL quenching effect observed, though the Y-scale is too large to allow sensing traces at low analyte levels distinguishable. As understood previously, the PL enhancement upon HC exposure is believed to arise from passivation of non-radiative surface states of the QDs.

From Fig. 42, sensing characteristics of absolute and relative or normalized PL changes as a function of xylenes concentration, calculated after subtraction of decreasing baseline, are compared in Fig. 43 and 44, respectively. Interesting is that the sensing performances of the QDs with PHA and PBA toward xylenes exposure are larger than those with PA and BA, analogs to their PL relation trend shown in Fig. 40. Their sensitivity values in Table 6 reported in two regions, below 2500 and above 4500 ppm xylenes indeed exhibit the same trend, i.e., the sensitivity values towards xylenes increases with the surface enhancing ligand length getting longer. However, upon inspection of Figure 44 it is apparent that the normalized PL changes in all four samples are approximately the same, suggesting the same sensing characteristics and mechanism pertain for all four samples.

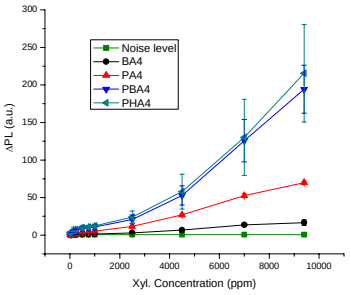

Fig.43 Absolute change in PL upon QD films exposure to Xylenes vs. HC concentration.

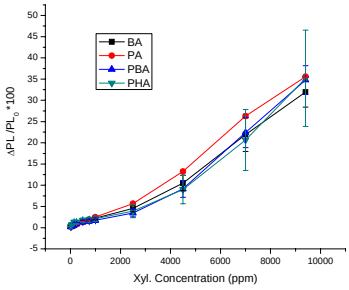

Fig.44 Normalized change in PL upon QD films exposure to Xylenes vs. HC concentration.

Table 6. Sensitivity values at low concentrations (below 2500 ppm) and high concentration(above 4500 ppm) of Xylenes.

Sample	Sensitivity toward Xyl. (15-2500 ppm) * 10^3	Sensitivity toward Xyl. (4500-9400 ppm) * 10^3
BA	1.0	2.0
PA	4.5	8.8
PBA	7.4	28.8
PHA	8.2	32.1

In summary, a higher quantum yield or PL from the QDs with the longest surface enhancing ligand, PHA, makes it more sensitive towards xylenes detection and a better candidate in designing the aromatic hydrocarbon optical sensors for this method. As discussed above, this is likely resulting from better surface state passivation effects with the longest ligand, producing the greatest signal change upon hydrocarbon exposure.

G. Gas sensors over large dynamic ranges with semiconductor quantum dots integrated onto nanotube arrays

As has been shown, before many applications can be realized, QDs must be functionally integrated into devices, and that requires control of their interactions and

spatial organization within a complex system. The controlled integration of functionally distinct QDs into hybrid structures appears to be an essential prerequisite for the realization of the high-performance optical and optoelectronic devices. Numerous attempts have been made in our group to fabricate nanoparticle-based films for sensing, including drop casting, co-polymerization of CdSe QDs and monomer, in-situ functionalization of QDs for layer-by-layer growth. Among them, drop casting method is proved to be capable to prepare workable QD sensing material with high HC sensitivity, for which the contributing factor is found to be rough and porous structure with the film. This initiates our development of novel sensor structure based on nanotechnology.

Here, we report the foremost gas sensing from CdSe/ZnS core/shell (Evident) or FBA modified CdSe core QDs dispersed on nearly ordered nanotube array of anodic aluminum oxide (AAO) template. This porous structure, as a quasi photonic crystal (PC) platform, both enhances QD PL signal and sensing response and suppresses wetting effects, proving to be a critical structural property for gas sensing. Commercially available AAO nanotube array template provides a simple approach to obtain QD based nanosensor without undesired QD agglomeration and enables the high performance of QDs.

The integration process involves selection of a suitable pore size to control the template surface hydrophobicity to be slightly less than QD solution, droplet size control (~ 6 mm), and slow self-assembly in a solvent vapor environment to get equilibrium QD dispersion. A comparison of Atomic Force Microscopy (AFM) images of AAO before and after QDs assemble, reveals that the QDs sit on the backbone of AAO without filling much in the pores (less than ~ 200 nm for blank AAO pore size), leaving the sample porous and rough as the desired structural property (Fig. 45). Surprisingly, the emission spectra shows that an AAO/QD (core/shell) sample placed on a Si support (blue) has ~8.4

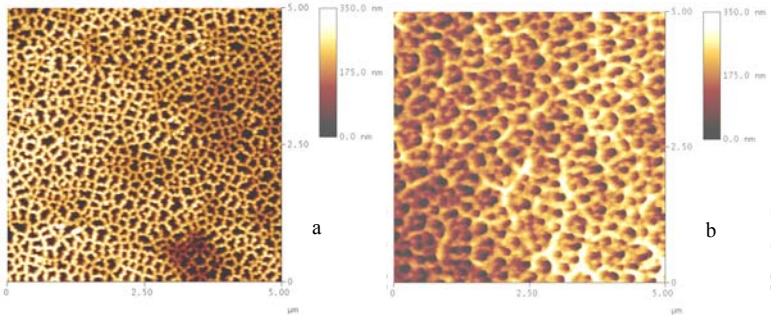

Fig. 45 Atomic Force Microscopy (AFM) images of (a) a blank anodic aluminum oxide (AAO) and (b) QD drop-cast AAO

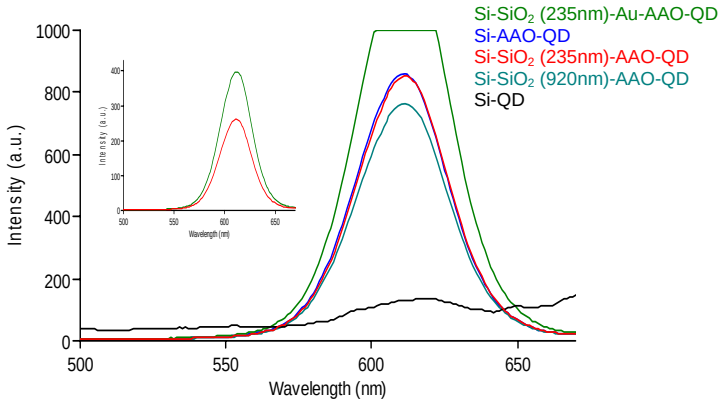

Fig.46 Photoluminescence spectra of the same AAO/QD sample placed on Si with SiO_2 and/or Au coatings and the sample of QD directly cast on Si. The inset is re-comparison in the presence / absence of Au layer after reduction of illumination intensity so that the signal is not saturated.

time stronger intensity than that of the same QD directly cast on Si (black) as shown in Fig. 46. The huge enhancement is owing to the introduction of AAO as discussed below, although there is some QD agglomeration induced PL quenching. When placing the same AAO/QD sample on Si with different surface coatings, we see again PL enhancement in the presence of Au layer (green, truncated) relative to that without Au layer (The inset is for a re-comparison between them with reduced illumination, indicating an enhancement ratio of ~1.5) and also see PL intensity variation with the thickness of SiO_2 layer on Si. This means that PL of AAO/QD sample can be further enhanced with manipulating the surface coating on the Si support, which is important to improving gas sensitivity as presented later. Fully in agreement with the result shown in Fig. 46 is that UV excited fluorescence pictures of three reproducible AAO/QD samples placed on a Si demonstrate intense colors over that of QD directly cast on a Si (Fig. 47b). The white light pictures of the samples are shown in Fig. 47a for a comparison.

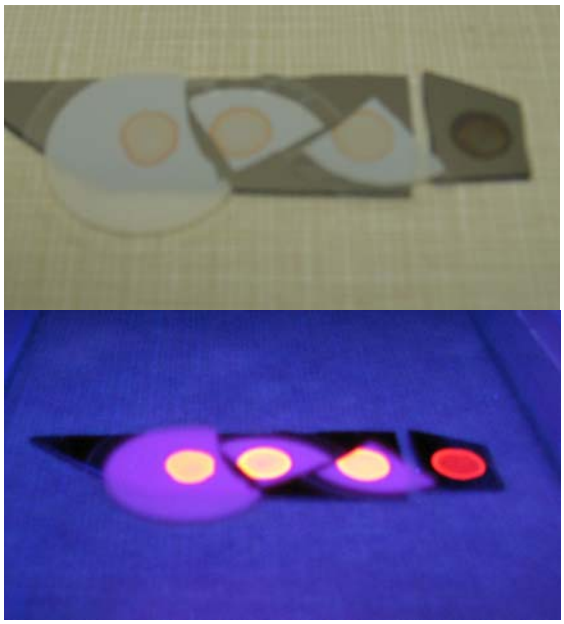

Fig. 47 (a) White light and (b) UV fluorescence pictures of three reproducible AAO/QD samples

The intensification of PL of QD by AAO verifies our previous method of creating rough films for enhancing PL and responses and is explained by the effect of AAO as a 2-D quasi-photonic crystal to redistribute local electromagnetic field of incident light for enhancing excitation or absorption by QDs and to realize efficient collection of QD emission by surface roughness enhanced scattering, according to the studies reported in the literature. The observed purple color of from the fluorescence picture of bare AAO substrate area (Fig. 47b) provides a direct evidence of such surface diffused scattering of incident UV light and redistribution of enhanced near-filed on the AAO surface. In contrast, there is no "color" seen on the silicon, where incident UV light is absorbed and specularly reflected.

The PL enhancement with Au layer results from noble metal nanoparticle associated surface plasmon resonance (SPR) enhanced re-absorption by QDs, while that with selected thickness of SiO_2 coating (e.g., 235 nm) reflects an optical interference effect from the underneath layers, i.e., 1-D photonic crystal effect.

Further more, with the introduction of porous AAO platform, PL of a Si/AAO/QD (core dots) sample reversibly enhances upon exposure to 9400 ppm xylenes in air (Fig. 48a), meaning that the PL quenching problem from previous Si/QD-PMMA samples as shown in Fig. 48b is completely suppressed at such a high analyte concentration. Thus, with this new sample structure, peak PL intensity enhancement prevails over the entire dynamic range, 15 – 9400 ppm xylenes (see Fig. 49 for baseline corrected sensing trace to xylenes exposure), without wetting effect induced competing PL quenching and non-

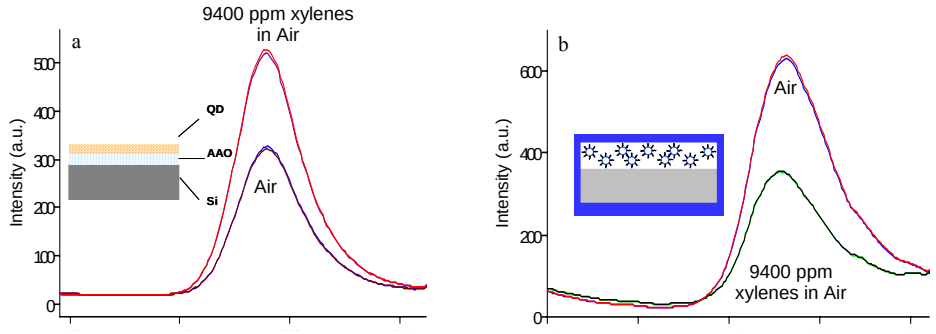

Fig. 28 (a) PL enhancement from Si/AAO/QD in contrast to (b) PL quenching from Si/QD embedded PMMA exposed to 9400 ppm xylenes

monotonic sensing described previously, qualifying a prerequisite for sensing application in real word. The suppression of PL quenching is owing to the retardation of an analyte wetting layer from formation on the QD dispersed nanopore array when exposed increased levels of analytes. The observed 10-15 ppm detection limit (see one more below) for xylenes defined with a signal/nose ratio of 2 as a criteria is still the lowest within QD based sensing results reported in the literature.

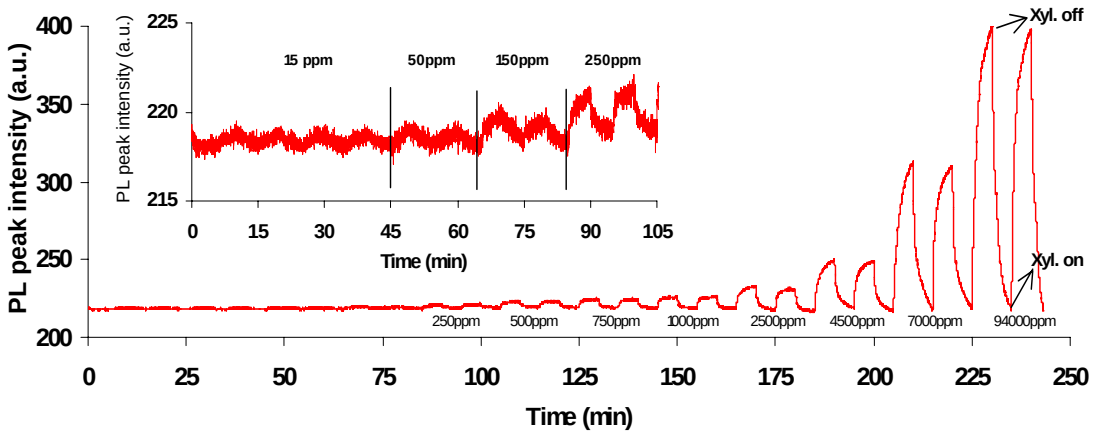

Fig. 49 Xylenes sensing trace of an AAO/QD (core) sample placed on Si

Sensing tests of a Si/AAO/QD sample for exposures of different HC species, benzene, toluene, and xylenes (BTX) reveal a similar sensing characteristic of peak PL intensity change as a function of analyte concentration for all the species (Fig. 50). The difference is that the sensing signal for xylenes is overall larger than those of toluene and benzenes, such as, a factor of ~2.5 and ~ 4 larger than those of the later two at 2500ppm, suggesting an increased selectivity toward xylenes over toluene and benzene though there is a small

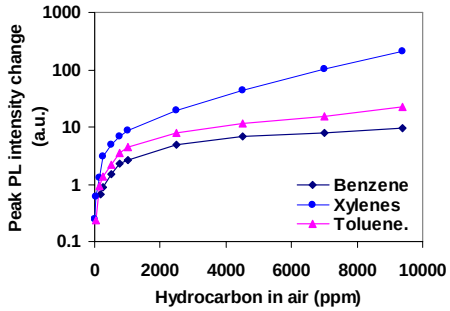

Fig.50 Benzene, toluene, and xylenes sensing characteristics of a Si/AAO/QD

uncertainty in actual concentrations of the analytes due to their different condensation coefficients. The observed selectivity is remarkable since the analytes differ by only one methyl group, which can be combined into smart senor array design to achieve a complete speciation sensing in future.

In accordance to the role of Au SPR for PL enhancement of AAO/QD (core/shell) sample, the presence of Au layer also enhances the sensing signal change of the sample across the entire exposed xylenes concentration range by a factor of, such as ~1.5 at

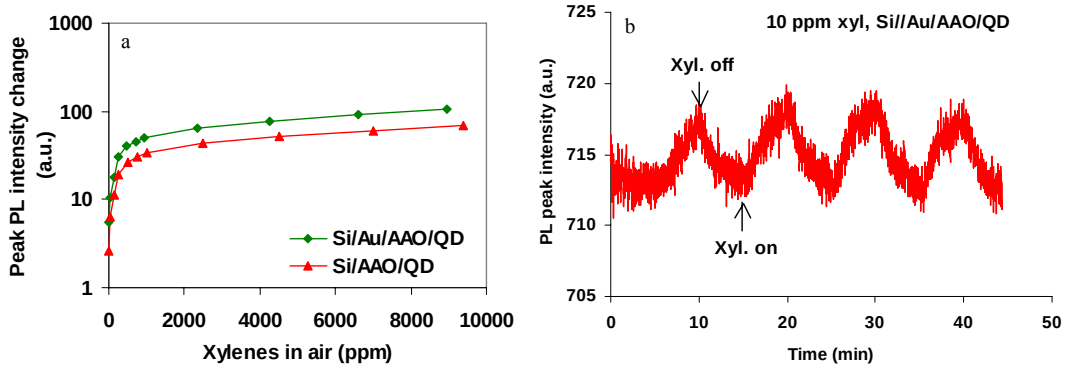

Fig. 51 (a) Comparison of xylenes sensing characteristics of QD samples with/without Au presence, (b) 10 ppm xylenes sensing trace of the Si/Au/AAO/Qd sample

~2500 ppm xylenes, relative to that in the absence of Au layer (Fig. 51a). The observed large signal change (~5.5 a.u. at 10 ppm xylenes) from the QDs with Au in the presence suggests a detection limit may be down to hundreds of ppb for xylenes (Fig. 51b). The results illustrate that both PL and PL based sensing performances of AAO/QD samples can be improved by tuning underneath supports and surface coatings.

Fig. 52a displays PL spectrum evolution of an AAO/QD (core/shell) sample during a time period of 252 days or more than 8 months. The sample was tested with dry air as a carrier gas and stored in ambient air without any protection measures. To our surprise, during such a long period, the PL just shows ~10 nm blue shift in peak position and a slow declining in peak intensity (Fig. 52b), due to photooxidation process persistent for any QDs. The months-long lifetime of our QD sensing materials is in significant contrast

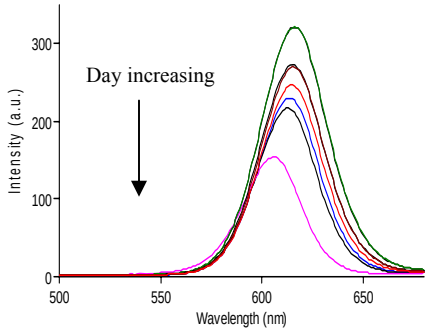

Fig. 52 (a) PL stability of an AAO/QD (core/shell) sample

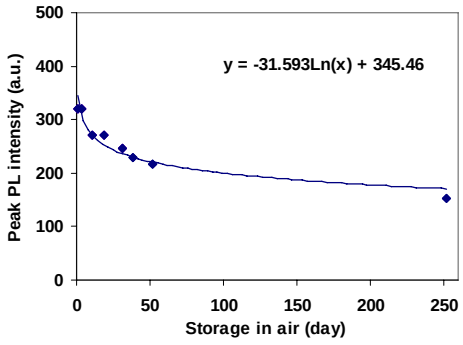

Fig. 52 (b) PL stability of an AAO/QD (core/shell) sample over a time period of 252 days

to days-long lifetime, which is typical of QDs when exposed to air without any polymer protection. Very encouraging is that the sensing performance of the sample is not impacted as revealed in Fig. 53, where the difference between the seemingly two groups of curves may result from the sample mounting.

The combination of QDs and nanotube array has enabled the development of QDs based materials for sensing applications across large dynamic ranges, for example, 10 to 9400 ppm for xylenes, which has been achieved for the first time in our group to our knowledge.

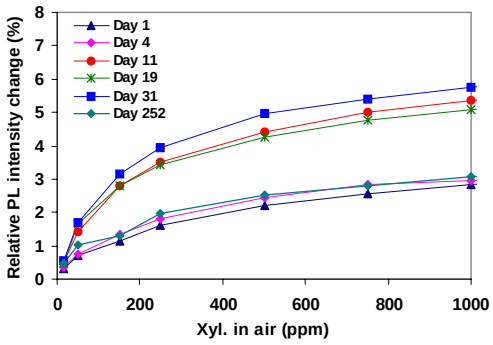

Fig. 53 Xylenes sensing performances of an AAO/QD (core/shell) sample over a time period of 252 days

4. Conclusions

Semiconductor quantum dots (QDs) have a potential for chemical sensing applications because of their high surface to volume ratio and unique size tunable properties like photoluminescence (PL). We proposed to surface functionalize CdSe quantum dots (QDs) during their synthesis process with aromatic surface modifying groups (BA, FBA, NA, PA, PBA, or PHA) to enhance their selective response towards the detection of toxic environmental species like benzene, toluene and xylenes aromatic hydrocarbons (HC). After incorporating the surface modified QDs into polymer such as PMMA to form nanocomposite porous and rough films on a silicon substrate by controlled drop casting, we have been able to achieve the lowest detection limit for HCs (e.g. ~10 - 15 ppm xylenes) within QD based sensing techniques. In addition, we observed 2-3 times greater selectivity for xylenes over that of toluene from FBA modified QDs based sensing material, likely owing to enhanced pi-pi stacking interaction in the presence of one more methyl group with xylenes. Both sensitivity and selectivity are found increasing with the type of the surface bound groups used in an order of bare, BA, NA and FBA. Also, a medium surface coverage is determined to be optimum for enhancing the sensing performance. However, we also observed PL quenching effect from these films with an increase in exposed HC concentrations, which competes with PL enhancement observed at low level of HC exposure, leading to undesired non-monotonic sensing characteristics over large dynamic analyte concentration ranges.

Meanwhile, we developed a method to do in-situ synthesis and polymerization of CdSe QDs with different monomers having a varied hydrocarbon side chain length and prepared clear QD/polymer nanocomposite films with QD uniformly dispersed in the matrices and PL properties retained. Though the films do not demonstrate promising sensing characteristics, the method may be useful for preparing QD materials for other applications and furthermore, integration of this layer by layer approach onto porous substrates might provide unprecedented control of both the chemistry and the sensing functionality. We explored fabrication of highly-ordered luminescent multilayered thin films of CdSe Quantum Dots. This is done by surface functionalization of CdSe QDs

during in-situ synthesis to afford stable and highly luminescent quantum dot solutions, followed by layer-by-layer formation of thin films comprised of the photoluminescent CdSe nanoparticles separated by long chain organic linkers between them and on surface chemically modified and functionalized glass or Si substrates. Such fabricated films are highly luminescent under UV illumination, clear and stable, and may be promising for different optical or optoelectronic applications even if they have not displayed good sensing performances yet. As a comparison, the controlled drop-casting proves to be a suitable method to fabricate workable QD/PMMA films for sensing test, the contributing factor for which is found to lie with a formation of a porous structure and rough surface of the film and resultant surface scattering enhanced optical absorption and emission by QDs.

We studied the sensing mechanism behind the inversion, desensitization and non-monotonic sensing behavior of the workable films and found that PL enhancement at low level HC exposure, similar to all that observed in liquid phase, results from intrinsic interaction between CdSe QDs and analytes, while PL quenching with an increase in HC concentration is attributed to high amount of HC absorption in the film and subsequent wetting/refractive index change reduced scattering effect and light absorption by QDs. HC approach to or adsorption on QD surface is considered to enhance surface passivation facilitated with photolysis process since PL response is found proportional to PL amplitude, thus leading to PL enhancement in the QD and analyte interaction process.

The contributing rough structure property we found inspired our development of a novel nanotechnology based method for fabrication of QD sensing materials by integration of CdSe QDs directly onto anodic aluminum oxide (AAO) platform as a quasi photonic crystal (PC) to increase PL intensity (a factor of 8.4 for example). Two fold merits of AAO nanotube array are: first, the rough surface or PC redistributes local electromagnetic field of incident light for enhancing QD excition and also allows effective collection of the resulting QD emission by surface scattering effect; second, the nanopores retard the wetting layer from formation on the sample surface, allowing PL enhancement based monotonic HC sensing over large dynamic range. Both PL intensity and responses are further improved with manipulating the coatings on the underneath Si support, such as, a factor of 1.5 enhancement with Au coating. PL change of ~5.6 a.u at ~10 ppm xylenes is observed, inferring a detection limit down to hundreds of ppb is possible. This is the lowest detection limit achieved within QD base results reported in the literature. PL and sensing performance has also been found to increase with selection of different type of surface bound groups, such as the one providing the longest distance from the phenol group it carries to the QD surface.

The combination of QDs and nanotube array has enabled the development of QDs based materials for sensing applications across large dynamic ranges, for example, 10 to 9400 ppm for xylenes, which has been reported for the first time to our knowledge. The further development by smart sensor design with creating optical spot array of QD with different sizes on nanotube template incorporating temperature gradient is expected to proved gas detection in highly speciation and sensitive manner.

References

[1] New York State Department of Environmental Conservation, "New York State Inactive Hazardous Waste Disposal Site Remedial Plan: 2000 Report", www.dec.state.ny.us.
[2]J. Hewett, NYS-DOT, Private Communication
[3] A. P. Alivisatos, *Science*, 1996, 271, 933-937.
[4] A. P. Alivisatos, *J. Phys. Chem.*, 1996, 100, 13226-13239.
[5] A. Henglein, *Chem. Rev.*, 1989, 89, 1861-1873.
[6] M. A. El-Sayed, *Acc. Chem. Res.*, 2004, 37, 326-333.
[7] M. Nirmal, L. Brus, *Acc. Chem. Res.*, 1999, 32, 407-414.
[8] A. J. Nozik, *Physica E*, 2002, 14, 115-120.
[9] T. Baron, A. Fernandes, J. F. Damlencourt, B. De Salvo, F. Martin, F. Mazen, S. Haukka, *Appl. Phys. Lett.*, 2003, 82, 4151-4153.
[10] M. Y. Han, X. H. Gao, J. Z. Su, S. Nie, *Nature Biotechnol.*, 2001, 19, 631-635.
[11] S. Coe, W. K. Woo, M. G. Bawendi, V. Bulovic, *Nature*, 2002, 420, 800-803.
[12] O. V. Vassiltsova, Z. Zhao, M. A. Petrukhina, M. A. Carpenter, *Sensors and Actuators, B: Chemical B*, 2007, 123, 522-529.
[13] Z. Zhao, M. Arrandale, O. V. Vassiltsova, M. A. Petrukhina, M. A. Carpenter, *Proc. IMechE. J. Nanoengineering and Nanosystems*, 2008, 221, 73-79.
[14] A. R. Clapp, I. L. Medintz, J. M. Mauro, B. R. Fisher, M. G. Bawendi, H. Mattoussi, *J. Am. Chem. Soc.*, 2004, 126, 301-310.
[15] L. Qu, X. Peng, Control of photoluminescence properties of CdSe nanocrystals in growth, J. Am. Chem. Soc. 124 (2002) 2049-2055.
[16] M. Kuno, J. K. Lee, B. O. Dabbousi, F. V. Mikulec, M. G. Bawendi, The band edge luminescence of surface modified CdSe nanocrystallites: Probing the luminescing state, J. Chem. Phys. 106 (1997) 9869-9888.
[17] C. B. Murray, D. J. Norris, M. G. Bawendi, *J. Am. Chem. Soc.*, 1993, 115, 8706-8715.
[18] G. Kalyuzhny, R. W. Murray, *J. Phys. Chem. B*, 2005, 109, 7012-7021.
[19] Q. Wang, Y. Xu, X. Zhao, Y. Chang, Y. Liu, L. Jiang, J. Sharma, D.-K. Seo, H. Yan, *J. Am. Chem. Soc.*, 2007, 129, 6380-6381.
[20] H. Skaff, K. Sill, T. Emrick, J. Am. Chem. Soc. 126, 11322 (2004)
[21] F. Antolini, L. Di, M. Re, L. Tapfer, Cryst. Res. Technol. 40, 948 (2005)
[22] V. Zucolotto, K. M. Gattas-Asfura, T. Tumolo, A. C. Perinotto, P. A.Antunes, C. J. L. Constantino, M. Baptista, R. M. Leblanc, O. N. Oliveira, Appl. Surf. Sci. 246, 397 (2005)
[23] I. Sondi, O. Siiman, E. J. Matijevic, Coll. Interf. Sci. 275, 503 (2004)
[24] (a) M. An, J.-D. Hong, K.-S. Cho, S.-M. Yoon, E.-S. Lee, B. K. Kim, J.-Y. Choi, *Bull. Kor. Chem. Soc.*, 2006, 27, 1119-1120. (b) S. Srivastava, N. A. Kotov, *Acc. Chem. Res*. 2008, 41, 1831-1841.
[25] M. C. Neves, A. S. Pereira, M. Peres, A. Kholkin, T. Monteiro, T. Trindade, *Mater. Sci. Forum*, 2006, 514-516, 1111-1115.
[26] O. V. Vassiltsova, D. Jayez, Z. Zhao, M. A. Carpenter, M. A. Petrukhina
Synthesis of Nanocomposite Materials with Controlled Structures and Optical Emissions: Application of Various Methacrylate Polymers for CdSe Quantum Dot Encapsulation
Journal of Nanoscience and Nanotechnology - Accepted and in Press 2008
[27] Submitted
[28] To be submitted 1
[29] A.Y. Nazzal, L. Qu, X. Peng, M. Xiao, Photoactivated CdSe nanocrystals as nanosensors for gases, Nano Lett. 3 (2003) 819–822.
[30] R.A. Potyrailo, A.M. Leach, Selective gas nanosensors with multisize CdSe nanocrystal/polymer composite films and dynamic pattern recognition, Appl. Phys. Lett. 88 (2006) 134110/1-134110/3.
[31] Z. Zhao, M. Arrandale, O. V. Vassiltsova, M. A. Petrukhina, M. A. Carpenter, *Sensors and Actuators, B: Chemical B*, 2009, accepted
[32] To be submitted

[33] J. Lee, V. C. Sundar, J. R. Heine, M. G. Bawendi, K. F. Jensen, Full color emission from II-VI semiconductor quantum dot-polymer composite, Adv. Mater. 12 (2000) 1102-1105.
[34] H. Skaff, M. F. Ilker, E. B. Coughlin, T. Emrick, Preparation of cadmium selenide-polyolefin composites from functional phosphine oxides and ruthenium-based metathesis, J. Am. Chem. Soc. 124 (2002) 5729-5733.
[35] H. Skaff, Y. Lin, R. Tangirala, K. Breitenkamp, A. Boker, T. P. Russell, T. Emrick, Crosslinked capsules of quantum dots by interfacial assembly and ligand crosslinking, Adv. Mat. 17 (2005) 2082-2086.
[36] H. Skaff, K. Sill, T. Emrick, Quantum dots tailored with poly(para-phenylene vinylene), J. Am. Chem. Soc. 126 (2004) 11322-11325.
[37] P. Lin, Y. Shen, K. Tetz, Y. Fainman, PMMA quantum dots composites fabricated via use of pre-polymerization, Optics Express 13 (2005) 44-49.
[38] K. Sill, T. Emrick, Nitroxide-mediated radical polymerization from CdSe nanoparticles, Chem. Mater. 16 (2004) 1240-1243.
[39] S.-W. Kim, S. Kim, J. B. Tracy, A. Jasanoff, M. G. Bawendi, Phosphine oxide polymer for water-soluble nanoparticles, J. Am. Chem. Soc. 127 (2005) 4556-4557.
[40] B. Gierczyk, G. Wojciechowski, B. Brzezinski, E. Grech, G. Schroeder, Study of the decarboxylation mechanism of fluorobenzoic acids by strong N-bases, J. Phys. Org. Chem. 14 (2001) 691-696.
[41] D. H. Phillips, J. C. Schug, Luminescence from aromatic polymers, monomers, and dimers under high-energy electron excitation, J. Chem. Phys. 50 (1969) 3297-3306.
[42] S. Jeong, M. Achermann, J. Nanda, S. Ivanov, V. I. Klimov, J. A. Hollingsworth, Effect of the thiol-thiolate equilibrium on the photophysical properties of aqueous CdSe/ZnS nanocrystal quantum dots, J. Am. Chem. Soc. 127 (2005) 10126-10127.
[43] O. Kulakovich, N. Strekal, A. Yaroshevich, S. Maskevich, S. Gaponenko, I. Nabiev, U. Woggon, M. Artemyev, Enhanced Luminescence of CdSe Quantum Dots on Gold Colloids, Nano Lett. 2 (2002), 1449-1452.